



Ocean and Sea Ice SAF

Technical Note
SAF/OSI/KNMI/TEC/TN/163

Calibration and Validation of ASCAT Winds

Jeroen Verspeek, Marcos Portabella, Ad Stoffelen, Anton Verhoef

Version 3.0

26 March 2008

DOCUMENTATION CHANGE RECORD

Reference: SAF/OSI/KNMI/TEC/TN/163

| Issue / Revision : | Date : | Change : | Description : |
|---------------------------|---------------|-----------------|---|
| Version 0.9 | 2007-02-22 | | Draft version. |
| Version 1.0 | 2007-06-15 | Major | Adapted description and figures Adapted correction tables and monitoring tables |
| Version 2.0 | 2007-10-01 | Major | Adapted document to one- transponder calibrated data |
| Version 2.1 | 2007-10-22 | Minor | Title changed, minor adaptations |
| Version 3.0 | 2008-03-26 | Major | Adapted document to three- transponder calibrated data |

Summary

Based on the OSI SAF cone visualisation tools at KNMI and the CMOD5 wind sensitivity, calibration of the ASCAT scatterometer is checked. In this report we describe and evaluate normalisation corrections to the pre-operational L1b ASCAT backscatter data as provided by EUMETSAT based on their three transponder calibration campaign. Improved consistency in the KNMI corrections is found, suggesting improved L1b calibration. In the outer swath consistent large departures remain, which need checking against other ancillary geophysical data sources to gain confidence in their validity. Indeed, still the three-transponder calibrated ASCAT wind product shows very similar characteristics to the one-transponder calibrated ASCAT scatterometer wind product and meets the wind product requirements.

Deviations between scatterometer and Numerical Weather Prediction wind derived backscatter still show a significant improvement after correction. Without correction the difference ranges from +0.5 dB to -0.4 dB going from the inner side to the outer side of the swaths. Also, the three-transponder calibrated L1b data show smaller interbeam differences. After the scaling correction is applied the difference ranges from -0.1 dB to +0.5 dB and is almost identical for the one-transponder and three-transponder calibrated data.

The pre-operational OSI SAF ASCAT level 2 wind product stream runs at KNMI using the pre-validated ASCAT level 1b stream at 25 km sampling as input, and may be maintained without any significant effects on product quality. The new L1b σ^0 stream will be corrected using the new linear scaling factors in the transformed z domain, which correspond to addition factors in the logarithmic domain (dB). These changes correspond to slightly resetting the ASCAT instrument gain per beam and per Wind Vector Cell (WVC) in order to maintain the backscatter data consistency and wind product quality.

In concert with EUMETSAT more detailed aspects of the ASCAT scatterometer L1b product and L2 product are currently being tested as more calibrated ASCAT products become available.

Contents

| | |
|---|----|
| Summary | 3 |
| Contents..... | 4 |
| 1 Introduction | 5 |
| 2 Visual correction | 6 |
| 3 Wind speed bias correction | 8 |
| 4 Normalisation correction..... | 10 |
| 5 Total correction factors | 12 |
| 6 NWP backscatter comparison | 15 |
| 7 Wind statistics | 17 |
| 8 MLE statistics..... | 22 |
| 9 Conclusions | 24 |
| Appendix A1 – Visualisation correction factors | 25 |
| Appendix A2 – Wind speed bias correction tables | 26 |
| - relative wind speed sensitivity | 26 |
| - wind speed bias correction factors for ss | 28 |
| Appendix A3 – Normalisation correction tables..... | 29 |
| - PPF550 to PPF530 | 29 |
| - PPF530 to zzz..... | 30 |
| - zzz to zz..... | 31 |
| - zz to ss..... | 32 |
| Appendix A4 – Total correction tables | 33 |
| – total for PPF550..... | 33 |
| – total for PPF530..... | 34 |
| – total for zzz..... | 35 |
| Acronyms and abbreviations | 36 |
| References | 37 |

1 Introduction

A pre-operational OSI SAF ASCAT level 2 wind product stream is running at KNMI using the commissioning ASCAT L1b stream at 25 km sampling as input. The L1b σ^0 stream is corrected using linear scaling factors in the transformed z domain [STOFFELEN and ANDERSON 1997], corresponding to addition factors in the logarithmic domain (dB). These changes correspond to resetting the ASCAT instrument gain per beam and per Wind Vector Cell (WVC). The objective is set to reproduce wind distributions similar to those from the ERS scatterometer, which provides a transfer standard from the ERS to the ASCAT era.

The Advanced Scatterometer (ASCAT) [FIGA et al 2002] is part of the payload of the MetOp satellite series of which the first one, MetOp-A, has been successfully launched on 19 October 2006. ASCAT is a fan beam scatterometer with six fan beam antennae providing a swath of WVCs both to the left and right of the satellite subsatellite track. Each swath is thus illuminated by three beams and is divided into 21 WVCs of 25 km size, numbered from 1-42 from left to right across both swaths (when looking into the satellite propagation direction. [STOFFELEN and ANDERSON 1997] describe the so-called measurement space. In this space the three backscatter measurements are plotted along three axis, spanning the fore, mid and aft beam backscatter measurements. As the satellite propagates and the wind conditions on the ocean surface vary in each numbered WVC, the 3D measurement space will be filled. CMOD5 [HERSBACH et al 2007] describes the geophysical dependency of the backscatter measurements on the WVC-mean wind vector as derived from ERS scatterometer data. Since, this dependency involved two geophysical parameters, namely two orthogonal wind components (or wind speed and direction), the 3D measurement space is filled with measurements closely following a 2D surface [STOFFELEN and ANDERSON 1997]. This folded surface is conical and consists of two sheets, one sheet for when the wind vector blows against the mid beam pointing direction (upwind section) and one for an along mid beam pointing direction wind vector (downwind section). The knowledge on the position of this surface through the Geophysical Model Function, GMF, CMOD5 provides a powerful diagnostic capability for the calibration and validation of the ASCAT scatterometer, since the same geophysical dependency should apply for both the ERS and MetOp scatterometers.

Besides ocean calibration EUMETSAT relies on the rain forest response, the backscatter over ice and transponder measurements for ASCAT calibration [FIGA et al 2004]. In this report we explore ocean calibration. In this report we assume that the main challenge lies in setting the antenna pattern or gain settings of the six beams and explore normalisation corrections to the experimental L1b backscatter data as provided by EUMETSAT during the commissioning phase of MetOp.

EUMETSAT has provided several preliminary datasets during the MetOp commissioning:

- 1) from 19 October 2006 until 29 January 2007, denoted "ss" data;
- 2) from 30 January 2007 until 12 February 2007, denoted as "zz" data;
- 3) from 13 February 2007 until 10 October 2007. (latest configuration of the pre-validated L1b data stream denoted as "zzz" data)
- 4) from 10 October 2007 until March 2008. One-transponder calibrated data, denoted as "PPF530" data with reference to the level 1B processor software version. This data was previously denoted as "z4" data
- 5) from 28 February 2008 onwards. Three-transponder calibrated data on an experimental basis in parallel with the PPF530 data, denoted as "PPF550" data

For the latest change to three-transponder calibrated data two batches have been provided covering one week of parallel streams each:

Batch 1: orbit 7060 to 7109, date 2008-02-28 to 2008-03-03

Batch 2: orbit 7143 to 7225, date 2008-03-05 to 2008-03-11, synchronised data streams

In this document only the synchronized data from batch 2 is used. From March 2008 onwards the L1B software identifier is written in the BUFR message and is used for automatic determination of the applicable calibration correction table in the ASCAT Wind Data Processor (AWDP).

In sections 2, 3, 4 and 5 the correction based on a visual inspection of the measurement space, the wind bias correction, the normalisation correction, and the total correction factor are described respectively. In sections **Error! Reference source not found.**, 7 and 8, the ocean calibration results, the wind statistics, and the Maximum Likelihood Estimator (MLE) statistics are discussed, respectively. The conclusions and outlook are presented in section 9. Note that all correction tables are listed in appendix A1 to A4.

2 Visual correction

A first correction is done in order to match the cloud of ASCAT backscatter (σ°) triplets (corresponding to the fore, mid, and aft beams) to the CMOD5 geophysical model function (GMF) in the 3-D measurement space [HERSBACH et al, 2006]. We use the OSI SAF visualisation package [VERSPEEK 2006-2] to produce the plots in z-space, i.e., (z_{fore} , z_{aft} , z_{mid}) where $z=(\sigma^\circ)^{0.625}$ [STOFFELEN, 1998]. Figure 1 is an example of such a visualisation from ERS. The double cone surface of CMOD5 is depicted in blue. The measured data is shown as a cloud of black points around the cone surface

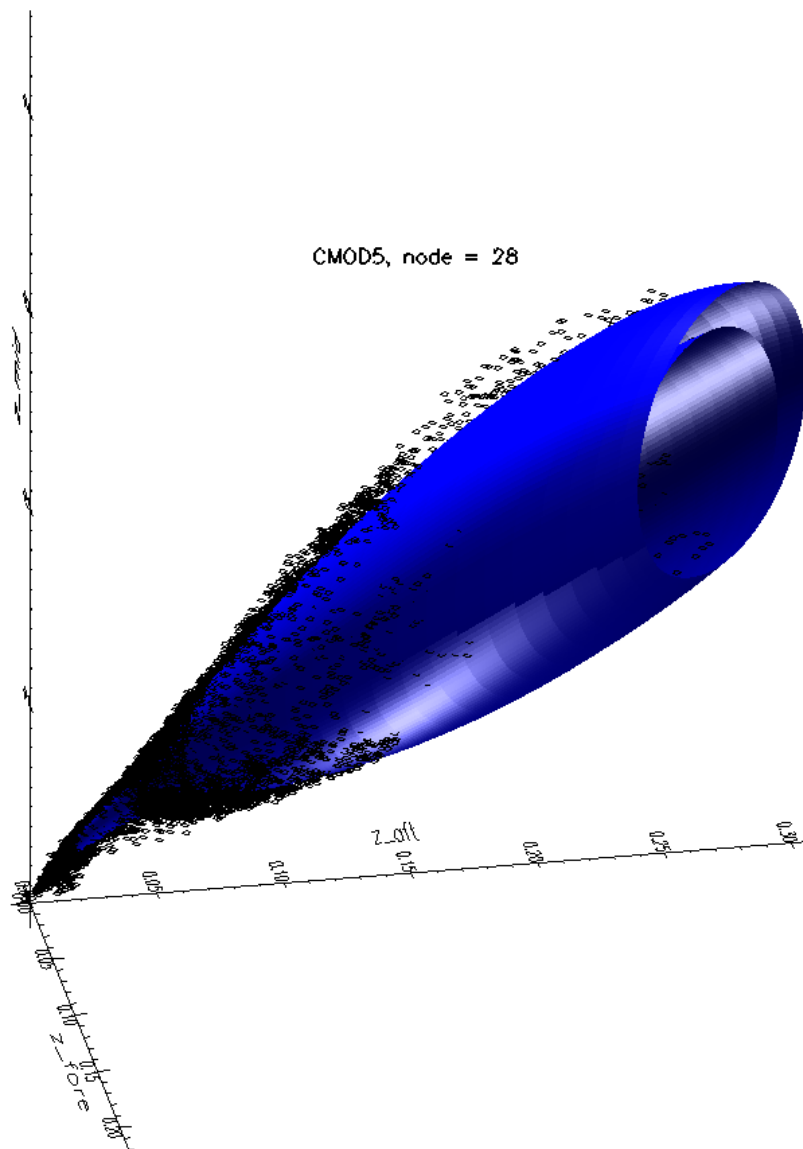


Figure 1 – CMOD5 wind cone with measured data points for WVC 28.

By looking at the projection of the wind cone on and data points in the proximity of the plane $z_{fore} = z_{aft}$, a normalisation factor for the mid beam is determined such that the CMOD5 cone by approximation fits the measurement points for each WVC. In the same way, by looking at a plot of the z_{fore} versus z_{aft} measurement points and the projection of the CMOD5 cone on the plane $z_{mid} = 0$, correction factors for the fore and aft beam are determined, such that the measurement points are distributed symmetrically. As such, the normalisation factors for the fore and aft beam are coupled in the following way:

$$z_{fore}^{corr} = 1/z_{aft}^{corr}$$

Equation 1

This deformation has the effect that the cloud of data points becomes symmetric, but does not correct correlated fore and aft beam biases.

The normalisation factors are determined per wind vector cell (WVC). See appendix A1 for the table of visual correction factors on the original EUMETSAT L1B data (ss).

Figure 2 shows the visualisation plots ($z_{fore}=z_{aft}$) for WVC 42 , i.e., the outer WVC of the right swath. Green points belong to the downwind sheet of the GMF cone surface, while purple points belong to the upwind sheet of the GMF surface. The retrieved wind is the wind solution that has a wind direction that is closest to the collocated NWP wind obtained from ECMWF. Figure 2a) shows uncorrected data from the original normalisation table (ss) and Figure 2b) shows the visual corrected data. Figure 2a) shows a clear discrepancy between data points and GMF, which is much improved in Figure 2b).

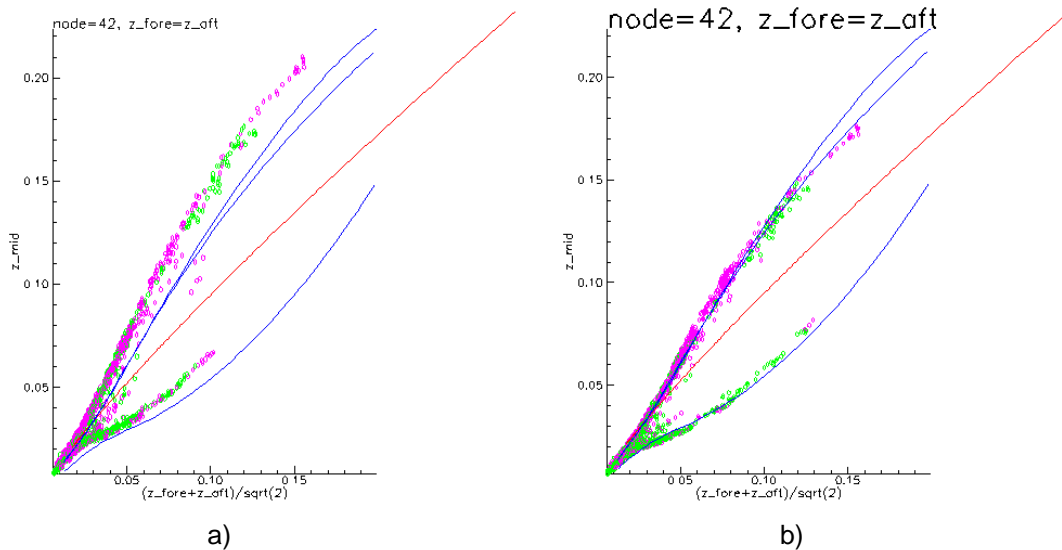


Figure 2 – CMOD5 wind cone (blue) and ice line (red) on the plane $z_{fore}=z_{aft}$, data points with 1 dB tolerance on either side of the plane.

- a) ss normalisation table, uncorrected data
- b) ss normalisation table, visual corrected data

Figure 3 shows the visualisation plots (projection on plane $z_{mid}=0$) for WVC 42. In Figure 3a) (uncorrected) the cloud of data points shows an asymmetry between z_{fore} and z_{aft} . The cloud seems to be rotated around the z_{mid} axis. Figure 3b) (visual corrected data) shows a more symmetrical distribution of data points with respect to the GMF.

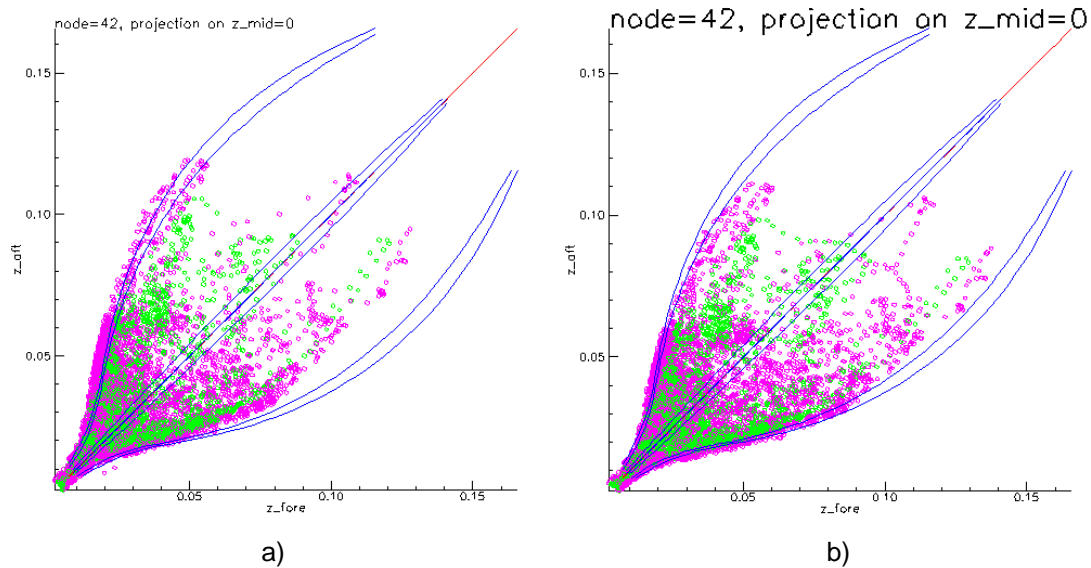


Figure 3 – Projection of the CMOD5 wind cone (blue), ice line (red) and data points on the plane $z_{\text{mid}}=0$
a) ss normalisation table, uncorrected data
b) ss normalisation table, visual corrected data

Note that the distribution of measurement points in figures 1-3 depends on:

- Kp noise;
- Beam collocation noise due to wind variability [PORTABELLA and STOFFELEN, 2006];
- The true underlying wind vector distribution that, for example, is far from uniform in wind direction.

It should be mentioned that all corrections are applied to the level 1b data before inversion with CMOD5.5 and ambiguity removal takes place in the level 2 processing. Thus the corrections will have influence on the quality control of each measured triplet.

3 Wind speed bias correction

After balancing the fore and aft beam for cone symmetry and bringing the mid beam measurements in line with the CMOD5 values on the cone, one degree of freedom remains in the normalisation of the cone. This degree of freedom lies in the translation of the cone along its major axis. Its first order effect is a wind speed bias after CMOD5 inversion, while effects on the misfit of the measurement triplets with respect to the cone surface are mainly second order. Therefore, a second normalisation is applied to correct for the remaining wind speed bias on top of the visual normalisation.

First the relative wind sensitivity is determined. It is defined as $(1/z) \cdot (dz/dV)$ and is taken at $V_0 = 8$ m/s because this gives a good approximation of the modal value, both for the wind speed and for the CMOD5 dz/dV derivative.

The z value is determined as an average over the CMOD5 upwind ($\phi = 0^\circ$), downwind ($\phi = 180^\circ$) and the two crosswind values ($\phi = 90^\circ$ and $\phi = 270^\circ$). Since CMOD5 is a second order harmonic in z space this provides the B_0 value. The derivative of z with respect to V , dz/dV is calculated using the central derivative approximation:

$$z_{ave}(\theta, V) = \frac{1}{4} \sum_{n=0}^3 z(\theta, V, \phi_n), \phi_n = 90^\circ \cdot n$$

Equation 2

$$(dz/dV)_{V=V_0} = \frac{z_{ave}(\theta, V_0+h) + z_{ave}(\theta, V_0-h)}{2h}$$

Equation 3

with $h = 0.1$ m/s. The wind speed bias is the difference between the retrieved wind and the first guess ECMWF NWP wind. This bias is multiplied with the relative wind sensitivity to get the wind bias normalisation factors. The correction factors are determined per WVC and per beam. See appendix A2 for tables related to the wind speed bias correction factors.

First guess ECMWF NWP winds are used as reference at this point, since the more precise triple collocation cal/val procedures require a year's worth of data, while only a limited set of ASCAT data has been available. ECMWF [HERSBACH, personal communication] reports that their routine operational comparison with buoys indicates that earlier low biases in the ECMWF winds have disappeared over recent time with the implementation of new ECMWF IFS model cycles.

CMOD5 winds were also found to be biased low [HERSBACH et al, 2007, PORTABELLA and STOFFELEN, 2007]. As such, all CMOD5 winds were corrected here to become 0.5 m/s stronger.

Figure 4 and Figure 5 show the same as Figure 2b and Figure 3b, respectively, but with the wind speed bias correction added to the visual correction. Note that the wind speed bias corrected data points (Figure 4 and Figure 5) are stretched away from the origin towards higher CMOD5 wind speed values as compared to the only visually corrected data points (Figure 2b and Figure 3b).

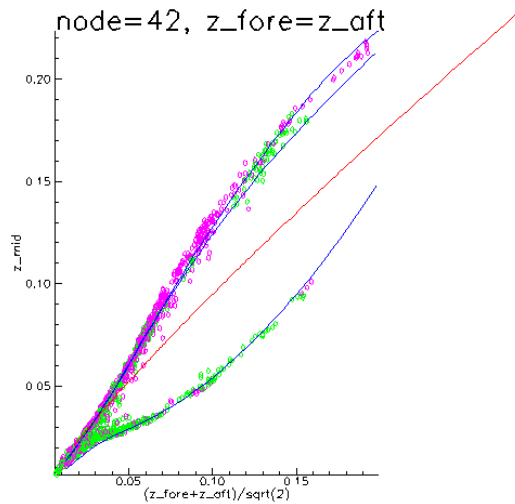


Figure 4 - Same as Figure 2b, but with the wind speed bias correction also applied.

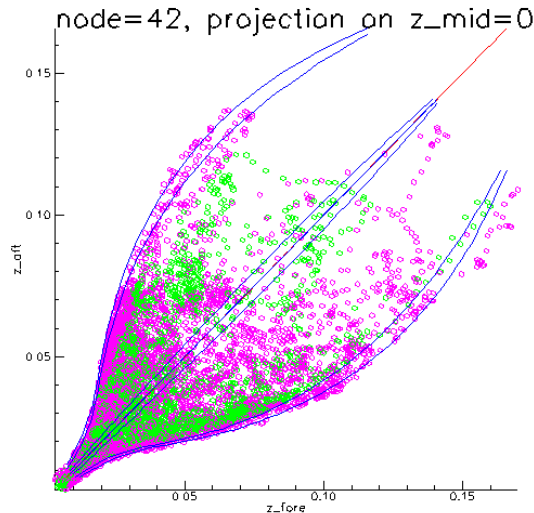


Figure 5 -Same as Figure 3b, but with the wind speed bias correction also applied.

4 Normalisation correction

A correction is applied to adapt the backscatter values in the three-transponder calibrated L1b stream. They are performed on the original data (denoted with ss). Later on, EUMETSAT several times improved their normalisation tables in the L1b processing. The normalisation factors are assumed to be multiplication factors in linear space, like the visual correction that we apply. Because all correction factors are linear, the corrections can be applied on top of each other. Normalisation correction tables are determined for each update of the L1b data. This is done by averaging the σ^0 differences in dB value from the new L1b data stream and the parallel original L1b data stream over one or more collocated orbits. The differences appear rather constant and show insignificant spread, confirming that the main effect in these conversions is a gain factor. Figure 6a) shows the average value per antenna and WVC of the difference in σ^0 value between the three-transponder calibrated L1b stream, hereafter referred as PPF550, and the one-transponder calibrated L1b stream PPF530. Figure 6b) shows the standard deviation (SD) for the correction as shown in Figure 6a). Only data from the second batch are used because these WVCs are synchronized. The first batch showed a shift in the acquisition time of PPF550 wind vector cells (WVCs) versus PPF530 WVCs of about 2 s, which corresponds to a lat/lon shift of about 10 km. For global comparisons like ocean calibration this shift is not relevant, but for a comparison on a Wind Vector Cell (WVC) basis, such as the one performed here, this subset of data cannot be used and is therefore filtered out from the first batch. In the synchronized batched no geographical dislocation is present and the data can be used for an assessment of the spread in the differences (SD). The differences show a smooth course. The differences are larger than in the previous L1b update but the SD show small values indicating that the pattern is persistent. For the inner swath WVCs 20-23 there is an increased SD for the mid antennas (yellow), but still an order of magnitude below the typical calibration changes. Also towards the outer side of the right swath the SD values of all three antennas are increasing but still have an acceptable value. This is compatible with all earlier ASCAT calibration changes, thus guaranteeing a constant-quality backscatter input to the L2 processing.

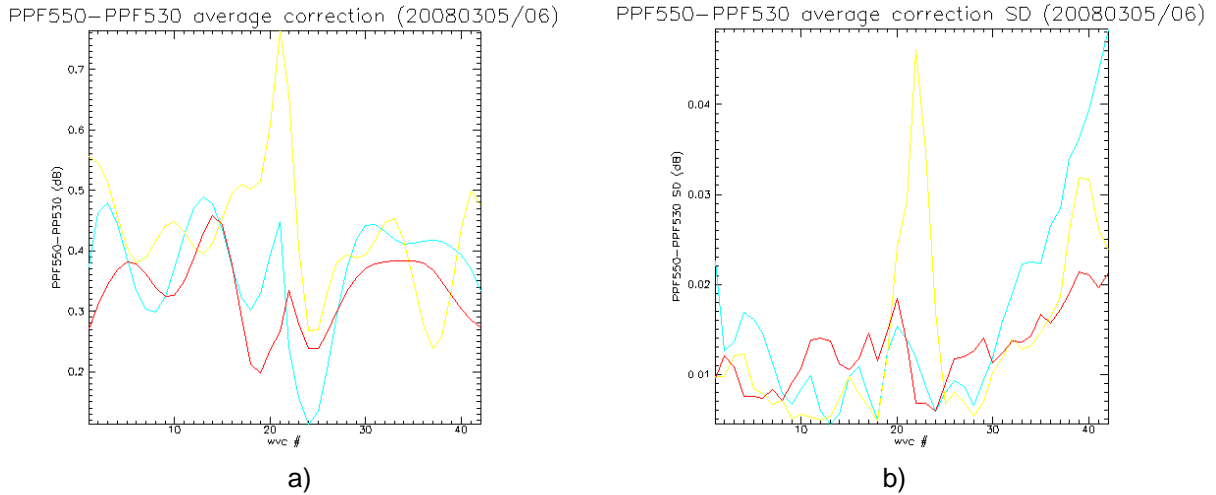
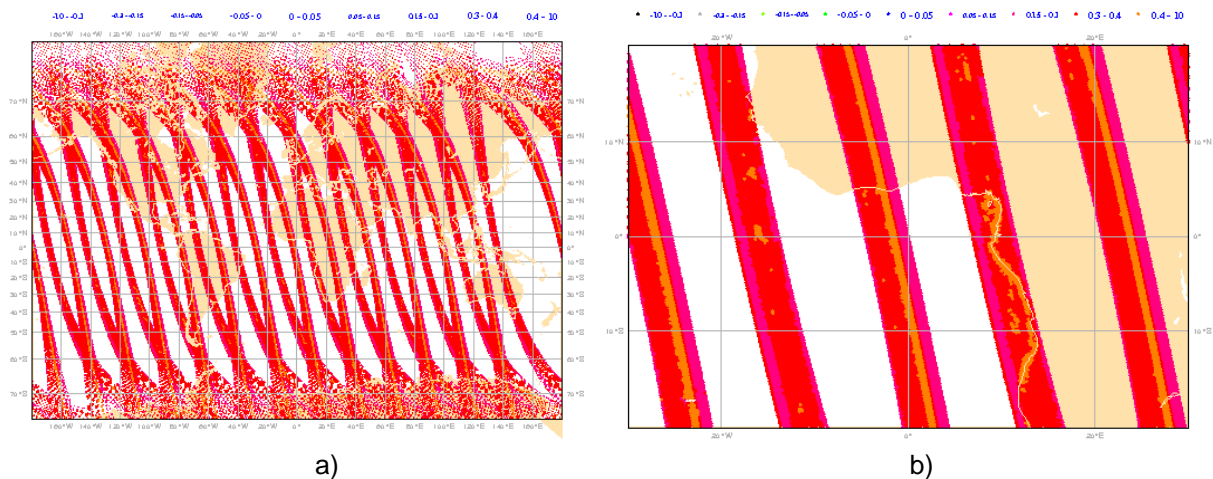


Figure 6 – Average difference and standard deviation of the three transponder calibrated (PPF550) and one transponder calibrated data (PPF530) from batch 2 (2008-03-05 / 2008-03-06)
 a) PPF550-PPF530 σ^0 difference in dB for the fore (red), mid (yellow) and aft (blue) antenna per WVC.
 b) standard deviation of the difference

Figure 7a) shows the difference for the fore antenna from the ascending part of the 13 orbits in the second batch on a world map. Figure 7b) shows a detail of the map in Figure 7a). Figure 7c) and Figure 7d) show the same data corrected for the average PPF550-PPF530 σ^0 difference as shown in Figure 6a). These orbits all have been checked for geographical dislocation between the two streams. No significant dislocation was found. Any dependency of the difference in backscatter on geographical location should be visible in these figures. The dependency appears to be mainly on WVC number or incidence angle. The orbits have a systematic pattern across the swath, showing the WVC dependency of the correction. Along the swath several structures can be seen, e.g., near the coastline. For other structures it is not clear beforehand where they originate from. Figure 7d) shows some dependency of the difference for the outer WVCs of the right swath for high latitudes. Overall, the corrections show no big systematic trends along the swath direction, and are thus largely independent of geographical location. However, local variations indeed appear in the order of the SD of the PPF550-PPF530 corrections. The other beams and calibration changes show similar corrections and SDs.



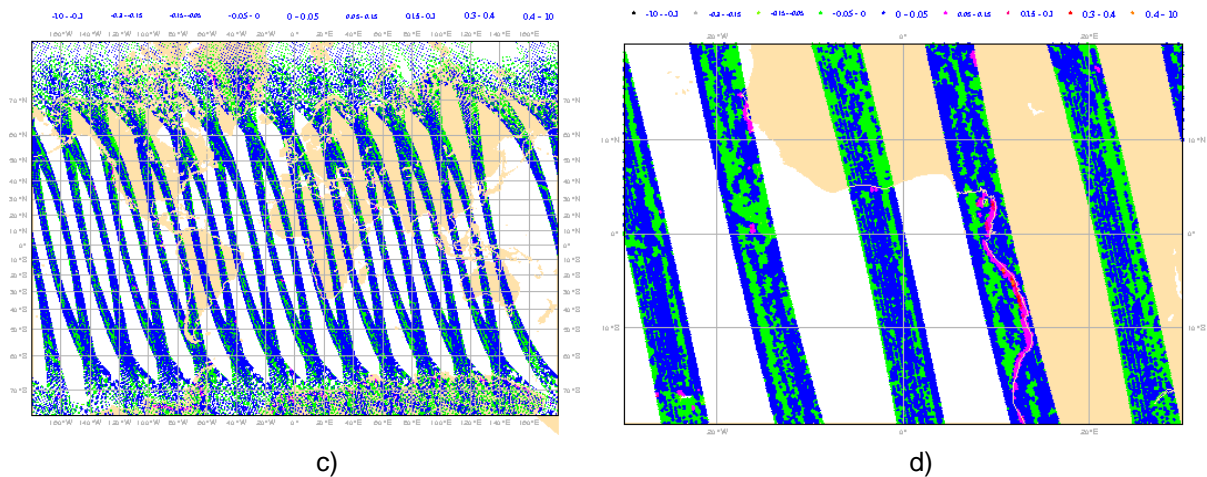


Figure 7 – Spatial plot of the average difference in σ^0 of the PPF550-PPF530 data for the fore antenna . Data from the ascending part of the 13 orbits in batch 2 is used (2008-03-05/2008-03-06)

- a) Global plot
- b) Detail plot (West-Africa)
- c) Global plot, deviations from the average values from figure Figure 6a)
- d) Detail plot (West-Africa), deviations from the average values from figure Figure 6a)

5 Total correction factors

A total correction is applied to adapt the backscatter values in the level 1b stream, which consists of the visualisation correction, the wind speed bias correction, and the normalization correction as discussed in sections 2, 3 and 4. In the following sections GMF version CMOD5.n is used in the ASCAT Wind Data Processor (AWDP) and the ocean calibration. CMOD5.n is a version of CMOD5 that is adapted for neutral winds. It is basically identical to CMOD5 with a 0.7 m/s shift in the input wind speed. The shape of the wind cone for CMOD5 and CMOD5.n is identical. The 28 fit-coefficients in the CMOD function have been recalculated for CMOD5.n by ECMWF, which lead to negligible deviations within the numerical precision of the fit procedure. The neutral wind speed GMF is the result of a triple collocation study with ECMWF winds and buoy winds [Portabella and Stoffelen 2007].

Figure 8a) shows CMOD5.n and the uncorrected PPF550 data for the plane $z_{fore} = z_{aft}$. Figure 8b) shows the same data after the total correction has been applied. The PPF550-data are transformed back to ss-data using the normalisation correction, and then the visualisation and wind speed bias corrections are applied. Figure 9 shows the same as Figure 8 but now for the projection of the wind cone and data points on the plane $z_{mid} = 0$. Figure 10 shows the intersection of the cone with the plane $z_{fore} + z_{aft} = 2z_{ref}$, for several values of z_{ref} , which correspond to (approximately) constant wind speed values. Also here the match between measurements and GMF is good. For other WVCs similar plots have been examined (not shown). For all examined WVCs the correspondence between data and model remains good.

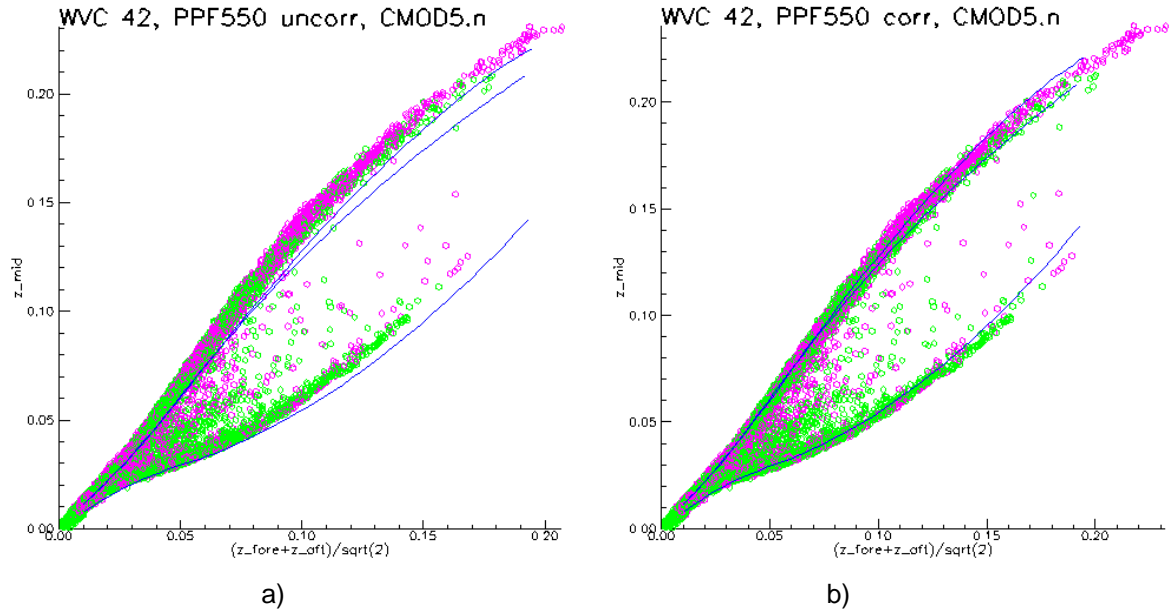


Figure 8 - Projection of the CMOD5.n wind cone (blue) and data points (green and purple) on the plane $z_{fore} = z_{aft}$. Data from 2nd batch
 a) PPF550 uncorrected data
 b) PPF550 with KNMI total correction applied

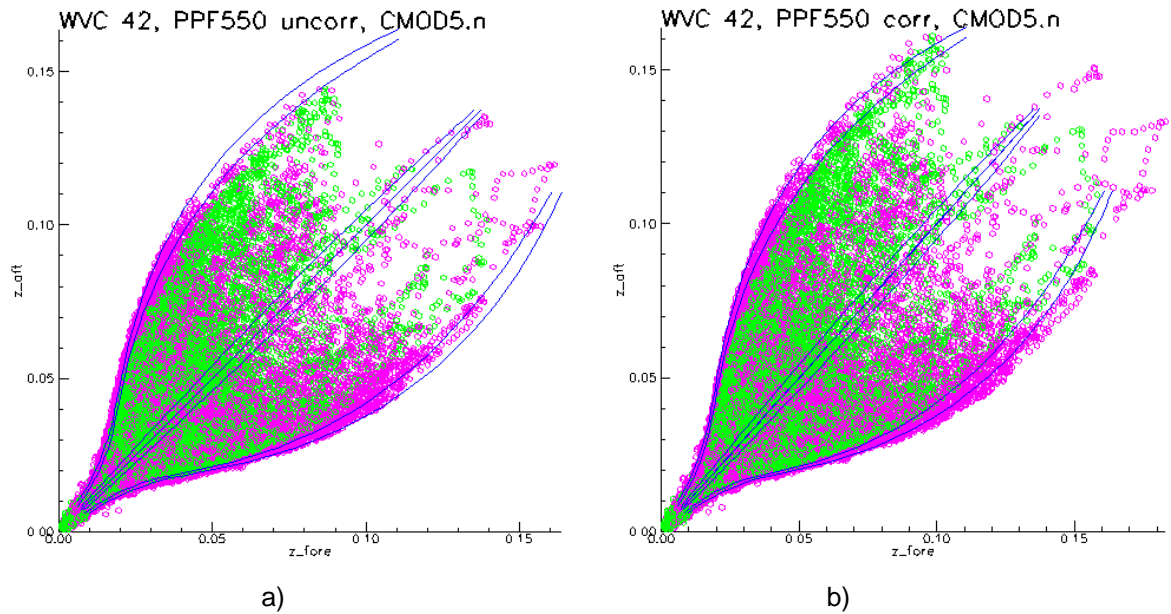


Figure 9 - Projection of the CMOD5 wind cone (blue) and data points (green and purple) on the plane $z_{mid} = 0$. Data from 2nd batch
 a) PPF550 uncorrected data
 b) PPF550 with KNMI total correction applied

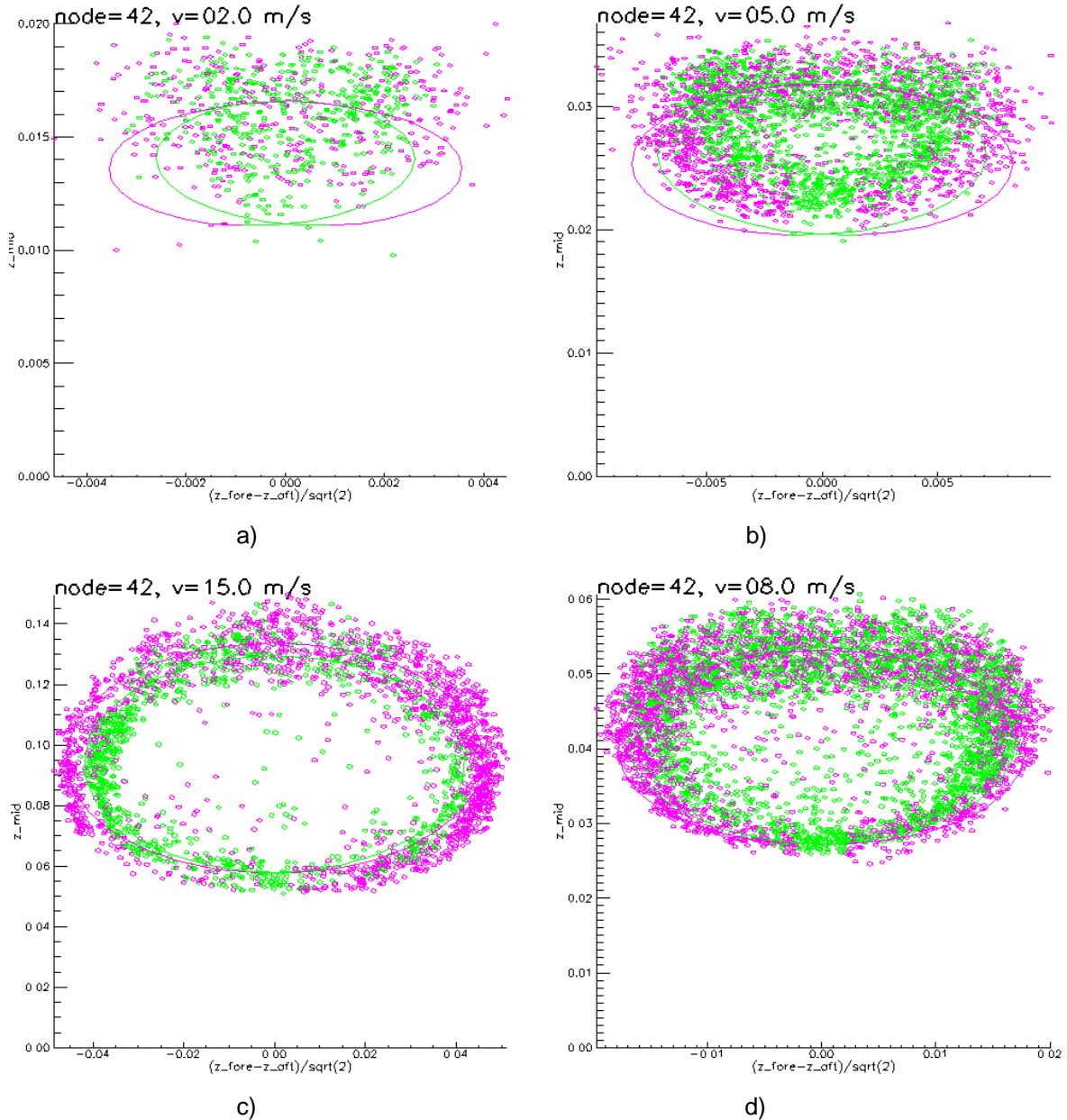


Figure 10 – Visualisation for WVC 42 of the corrected σ^0 triplets (coloured dots) and CMOD5.n (coloured ellipses), for several intersections of the cone with the plane $z_{fore} + z_{aft} = 2z_{ref.}$, corresponding to the following wind speeds:

a) $V = 2$ m/s b) $V = 5$ m/s c) $V = 8$ m/s d) $V = 15$ m/s

The correction factors are again determined per wind vector cell (WVC) and beam. See appendix A3 for normalisation correction factor tables.

Figure 11a) and b) show the total correction factor for the PPF530 and PPF550 data respectively. The correction from Figure 6a) has been added to the total correction factor for the PPF530 data in order to generate the total correction factors for the PPF550 data. The patterns look very consistent for all antennas. This is an indication that the inter-beam biases are small and that only an overall correction, which is basically incidence angle dependent, is needed. The corrections for PPF550 look even more consistent than for PPF530, thus showing a calibration improvement. For high incidence angles the correction is still large, i.e., above 1 dB. This may be caused by either a L1b calibration issue or a CMOD5 issue, since CMOD5 has not yet been validated for such high incidence angles. We suggest ancillary sea ice, rain forest and soil geophysical comparisons to gain confidence in the backscatter calibration in the outer swath..

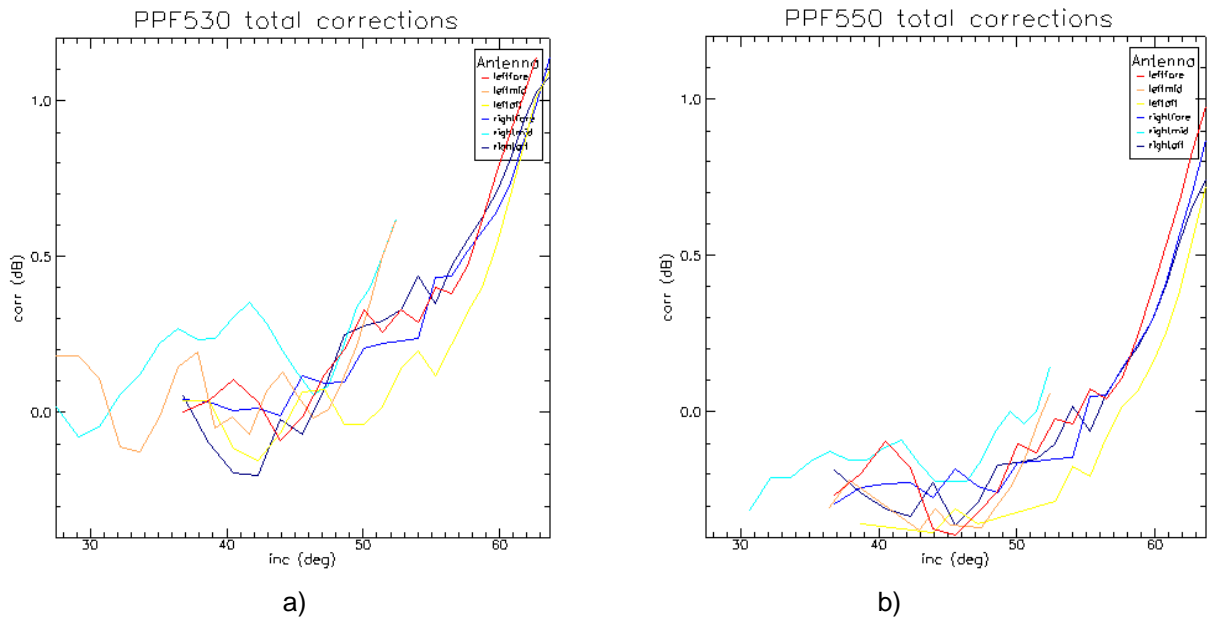


Figure 11 – Total correction factors per antenna and incidence angle
 a) PPF530 one-transponder calibrated data
 b) PPF550 three-transponder calibrated data

The tables with total correction factors can be found in appendix A4.

6 NWP backscatter comparison

A NWP simulated backscatter comparison [VERSPEEK 2006] is performed with the parallel L1b data streams PPF530 and PPF550, both for the corrected and uncorrected case. Both L1b products are processed with AWDP using 2D-VAR ambiguity removal to provide a level 2 product with scatterometer retrieved winds and collocated NWP winds from the ECWMF model. The data is conservatively filtered to exclude land and ice.

Figure 12 shows the results. Figure 12a) and Figure 12b) show the PPF530 and PPF550 uncorrected case where the difference between the measured averaged σ^0 values and the averaged σ^0 values simulated from the NWP winds is depicted. The difference ranges from +0.3 dB for to inner side to -0.8 dB for the outer side of the swath in Figure 12a), and from +0.6 dB to -0.4 dB in Figure 12b). Furthermore, the difference shows a systematic trend which tends to large negative values for all antennae. The interbeam bias is improved for the PPF550 case with respect to the PPF530 case, showing less difference between the antennae. There are still some wiggles remaining in the left mid beam response.

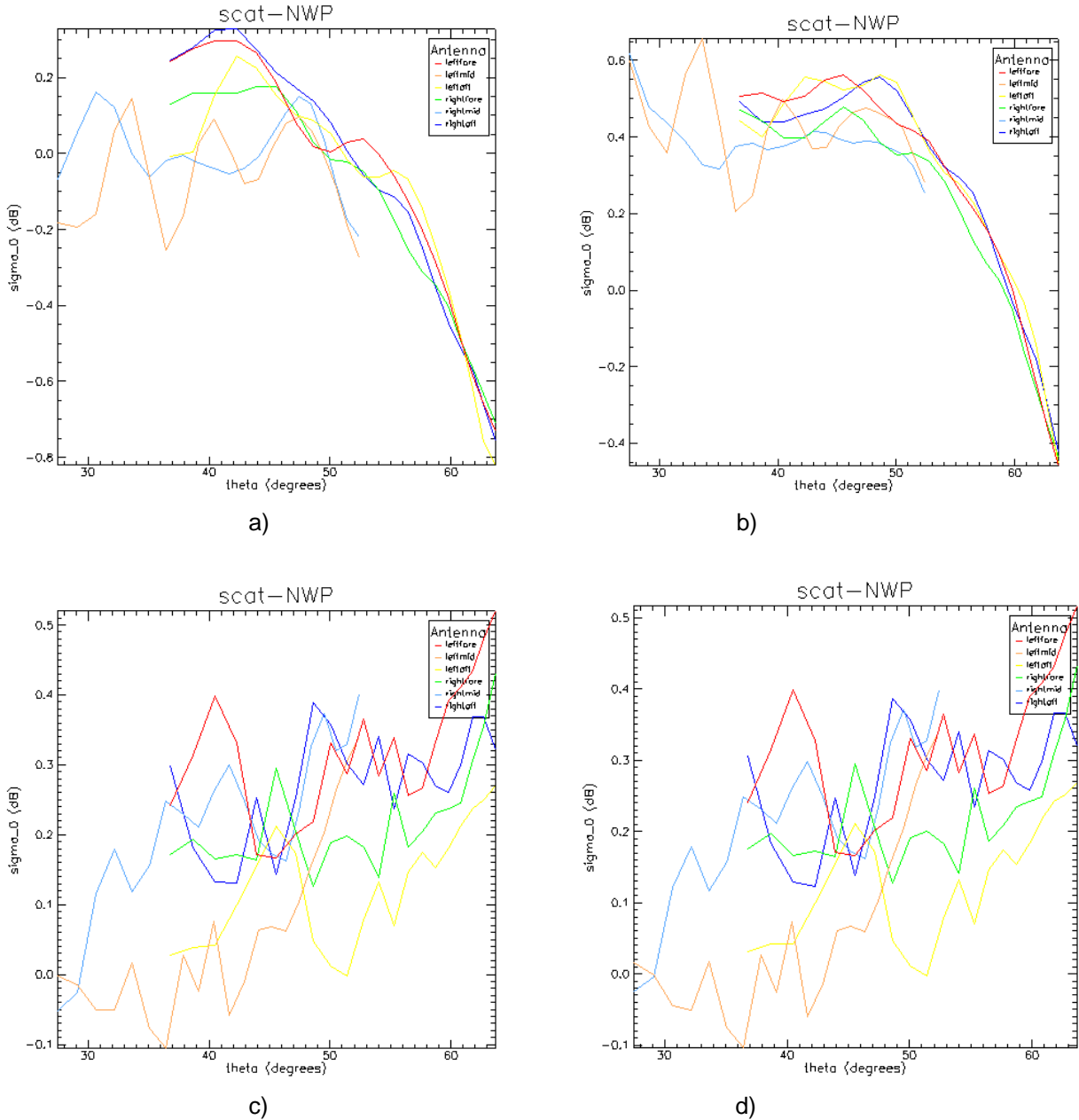


Figure 12 – NWP comparison results for the batch2 data from 2008-03-05. to 2008-03-06 of CMOD5.n backscatter values based on real ECMWF 10m winds with
 a) PPF530 data (uncorrected)
 b) PPF550 data (uncorrected)
 c) PPF530 data (corrected)
 d) PPF550 data (corrected)

For Figure 12c) and Figure 12d) the correction factors were applied to the L1b backscatter values. The difference ranges from -0.1 dB to +0.5 dB. This is a clear improvement with respect to the uncorrected cases. The σ_0 bias is in both cases around +0.2 dB. This corresponds to the fact that we use real 10-m ECMWF winds as input for CMOD5.n. When CMOD5.5 would have been used instead of CMOD5.n the bias would be 0.2 dB lower, so around zero. There is little systematic behaviour in the σ_0 bias. Only a slight increase with the incidence angle remains.

7 Wind statistics

In this section some statistical plots comparing ASCAT wind and ECMWF wind are given.

First of all it is of interest to look at differences between the PPF550 corrected and PPF530 corrected wind solutions. Because the PPF550 correction incorporates the average difference between PPF550 and PPF530, both wind solutions are expected to highly correlate and show only small differences. Figure 13a) shows a scatter plot of the wind vector differences for the two data streams for one orbit. The outliers can be clearly identified and are due to selection of the “other” solution by 2DVAR ambiguity removal at low winds. The number of outliers is in the order of a fraction of 0.001 of the total number. Figure 13b) shows the same plot but in a zoomed view. The points are centred around the origin with a standard deviation of 0.23 m/s in u and v direction.

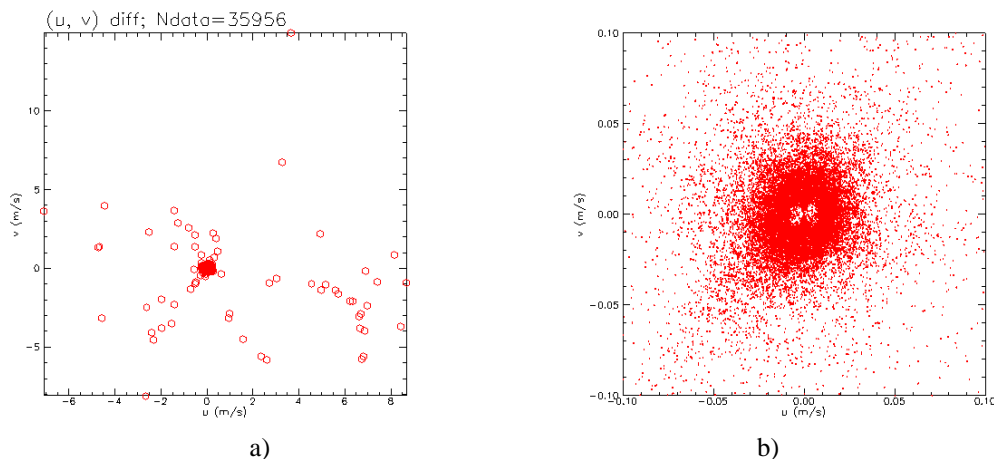


Figure 13 – Scatter plot of the wind vector difference of PPF550 corrected and PPF530 corrected solutions for one orbit of data.

a) wide view b) zoomed view

Figure 14 and Figure 15 show the wind statistics per WVC for PPF550 and PPF530 respectively.

Corrected data is represented in red, uncorrected data in orange. The statistics for the corrected data sets PPF550 and PPF530 are almost identical. This is to be expected because the PPF550-to-PPF530 correction is small and almost linear. The wind speed bias shown in Figure 15a) has an average value of 0.2 m/s for the corrected case. This is due to the fact that CMOD5.n is used while we compare to real ECMWF winds rather than to neutral winds. Neutral winds have a bias of 0.2 m/s with respect to real 10m winds.

For the uncorrected cases, already significant bias appears in WVCs in the projected ERS swath. The underscaled winds from the uncorrected set result in smaller wind speed SD in the outer swath, but a much larger wind direction SD than for the corrected set, as expected.

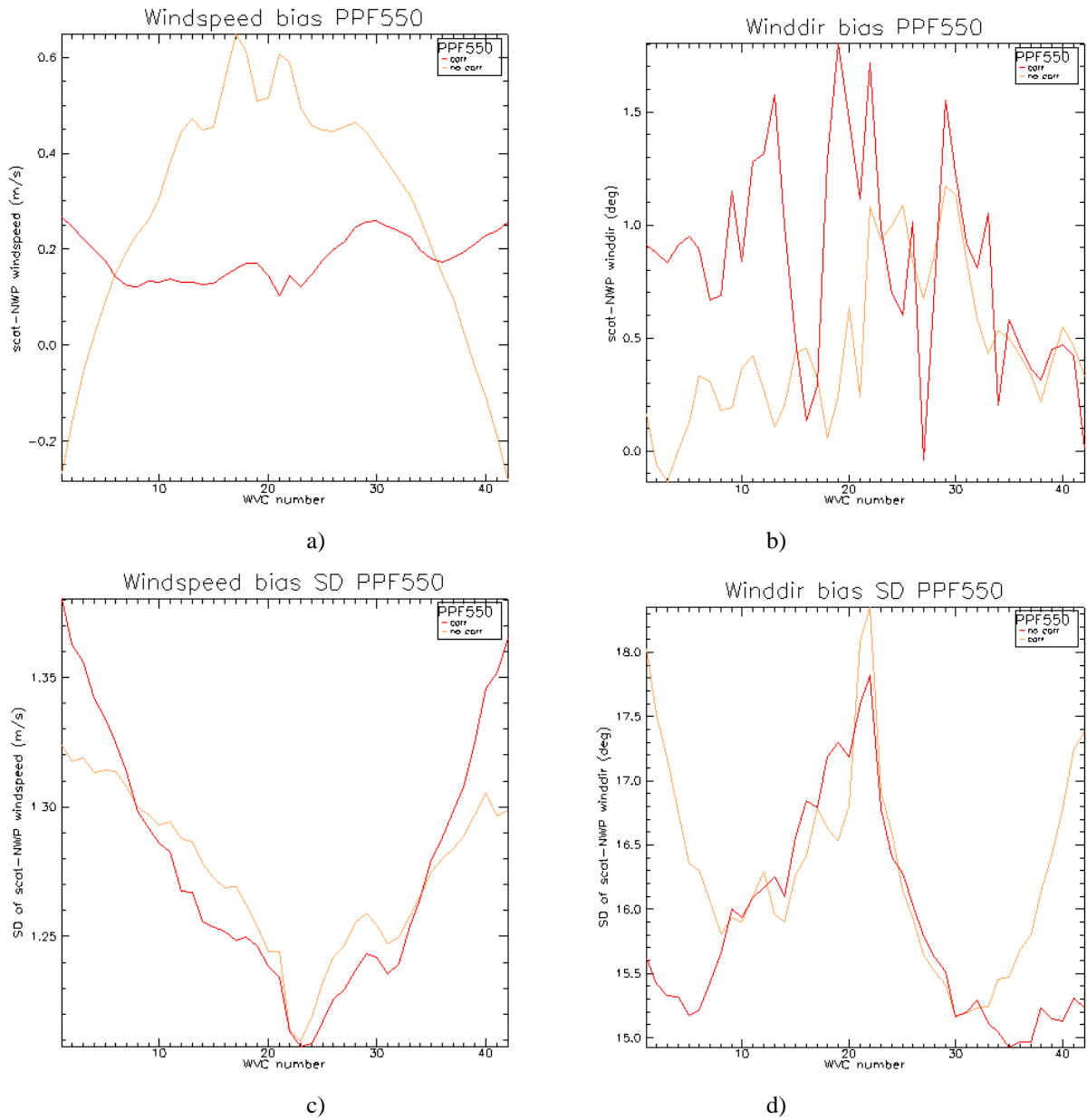


Figure 14 – Wind comparison per WVC between ASCAT and ECMWF for batch 2 (2008-03-05 / 2008-03-11), PPF550 corrected and uncorrected. Wind direction statistics are for the 2DVAR wind solutions for ECMWF winds larger than 4 m/s.

a) wind speed bias b) wind direction bias
 c) wind speed SD d) wind direction SD.

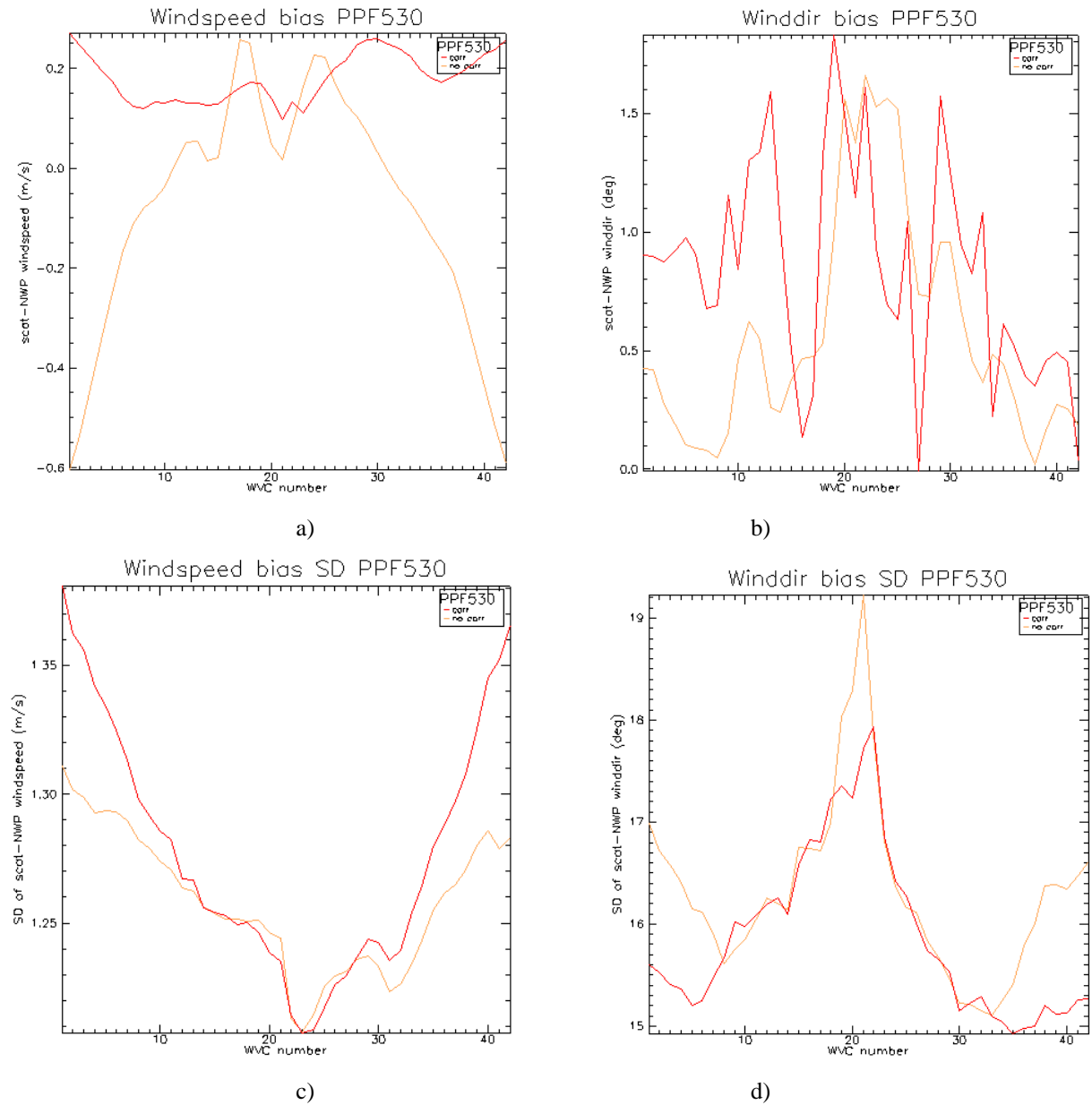


Figure 15 – Wind comparison per WVC between ASCAT and ECMWF for batch 2 (2008-03-05 / 2008-03-11), PPF550 corrected and uncorrected. Wind direction statistics are for the 2DVAR wind solutions for ECMWF winds larger than 4 m/s.

a) wind speed bias b) wind direction bias
 c) wind speed SD d) wind direction SD.

Figure 16 and Figure 17 show the wind scatter plots for the 2nd batch for corrected PPF550 and PPF530 data respectively. Only insignificant differences appear in the wind speed contour plots and the wind direction contour plots for ECMWF winds above 4 m/s. The corrected PPF550 and PPF530 data sets are statistically very similar in terms of wind performance, as may be expected from Figure 13.

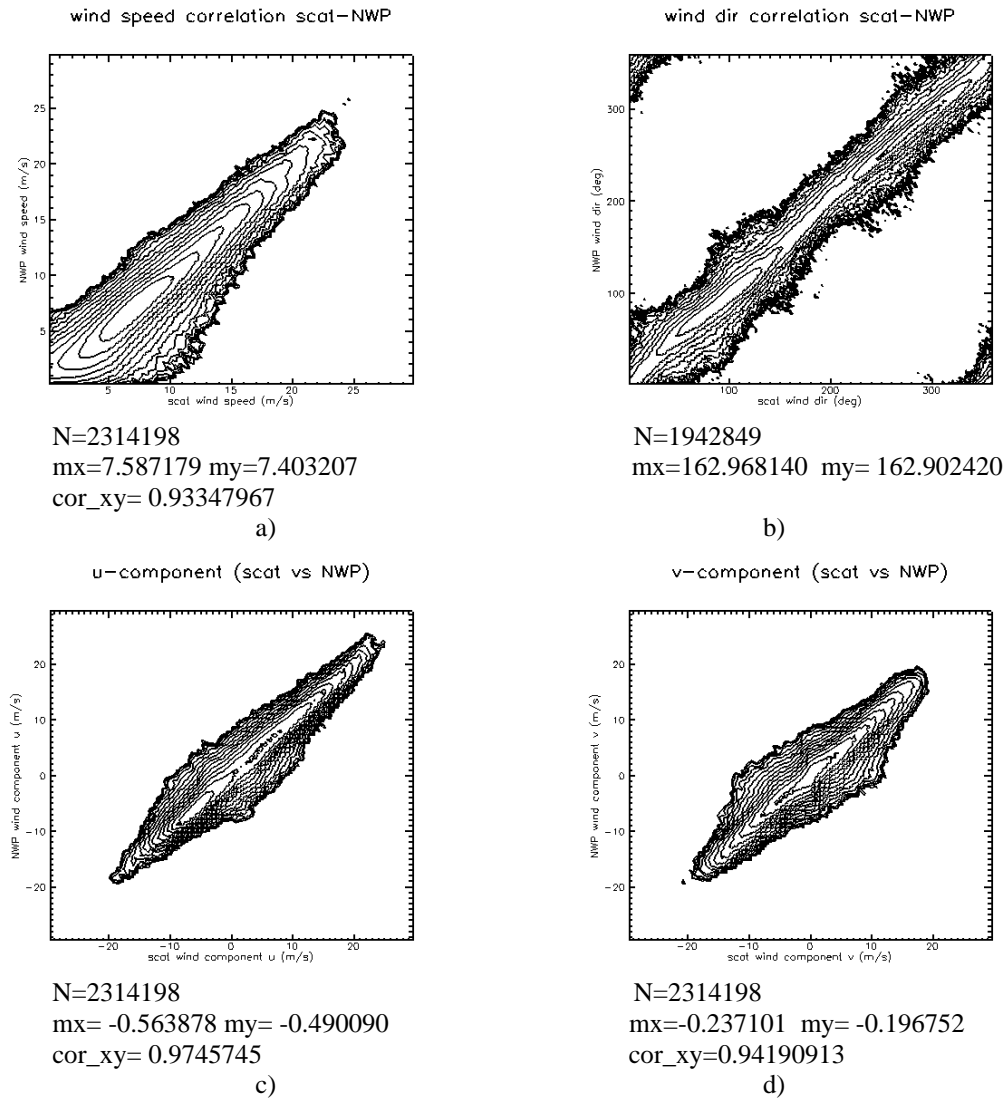


Figure 16 – Two-dimensional histogram of the 2D-VAR KNMI-retrieved wind solution versus ECMWF wind for all WVCs. The PPD550 three-transponder calibrated data from the 2nd batch after OSI SAF correction is used. N is the number of data; mx and my are the mean values along the x and y axis, respectively; and cor_xy is the correlation coefficient for the xy distribution. The contour lines are in logarithmic scale: each level up is a factor of 2. Lowest level=10, there are 15 levels in total.

a) wind speed (bins of 0.4 m/s) b) wind direction (bins of 2.5°) for ECMWF winds larger than 4 m/s.
c) wind component u (bins of 0.4 m/s) b) wind component v (bins of 0.4 m/s)

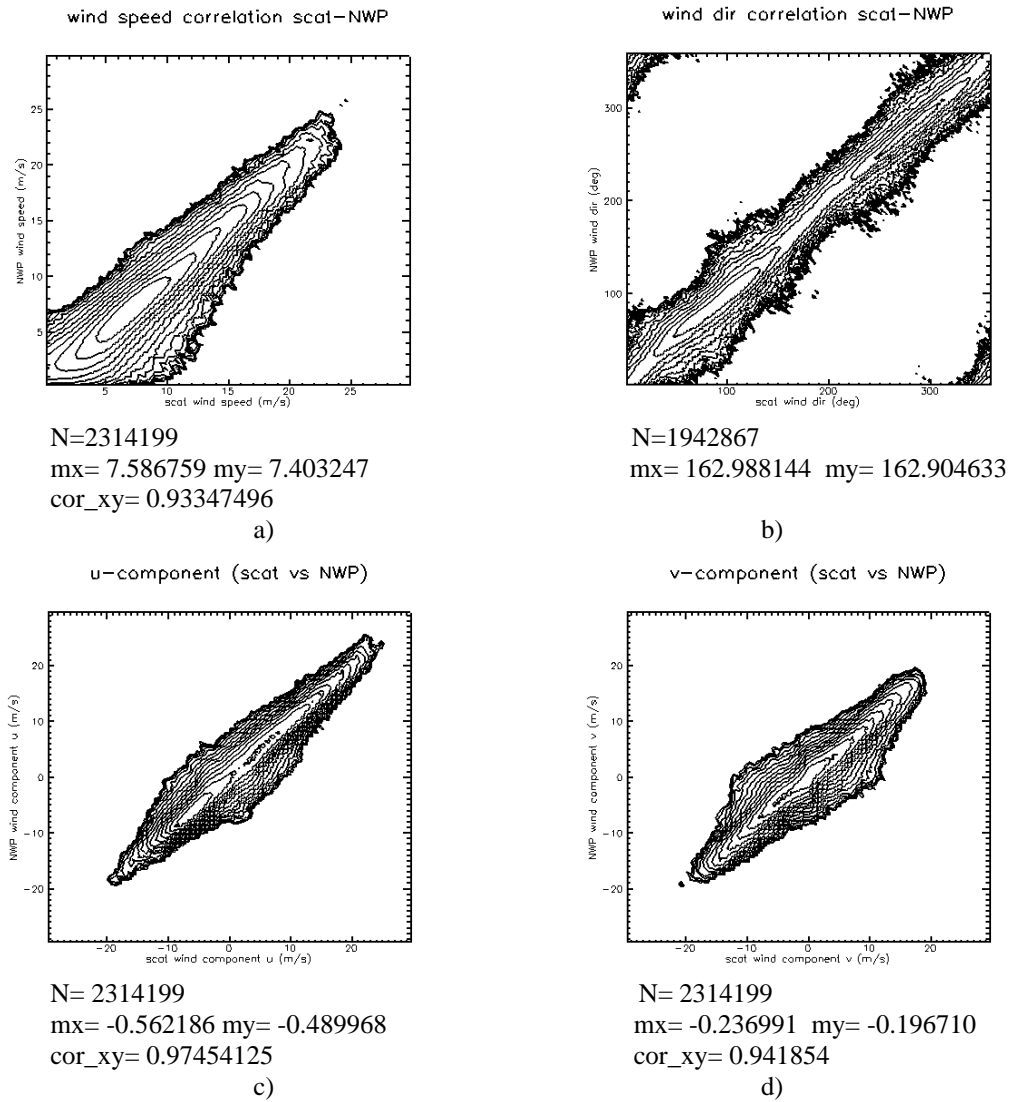


Figure 17 – Same as Figure 16 but now for the PPF530 operational data (corrected).

8 MLE statistics

Figure 18 shows the normalised distance to cone or Maximum Likelihood Estimator (MLE) [PORTABELLA and STOFFELEN 2006] as a function of WVC for the PPF550 corrected and uncorrected cases. It is clear that the corrected case shows larger accumulations at the origin, i.e., triplets are closer to the CMOD5 cone, as compared to the uncorrected. Furthermore the uncorrected case shows a clear systematic error. For the outermost WVCs the MLE shows more negative values, corresponding to points outside the cone. In the corrected case

Figure 18b) these systematic errors are not present anymore.

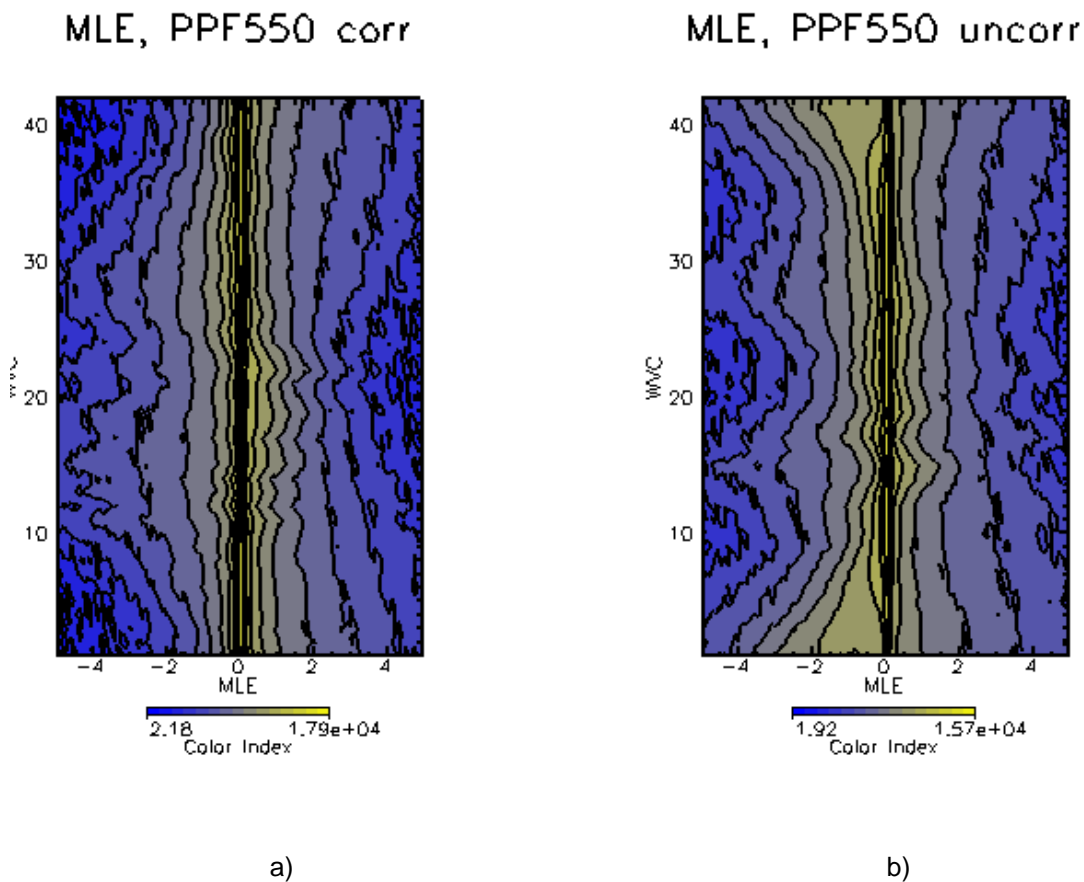
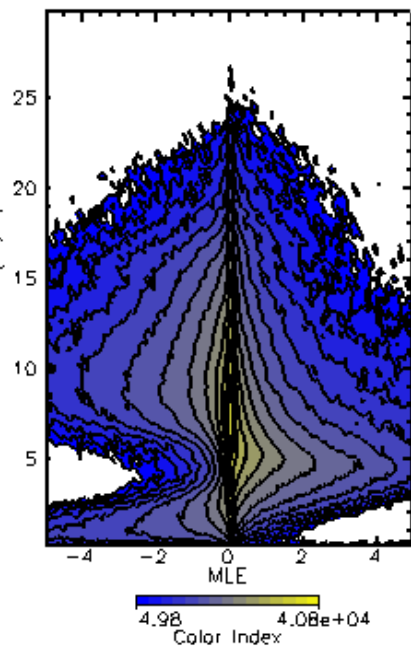


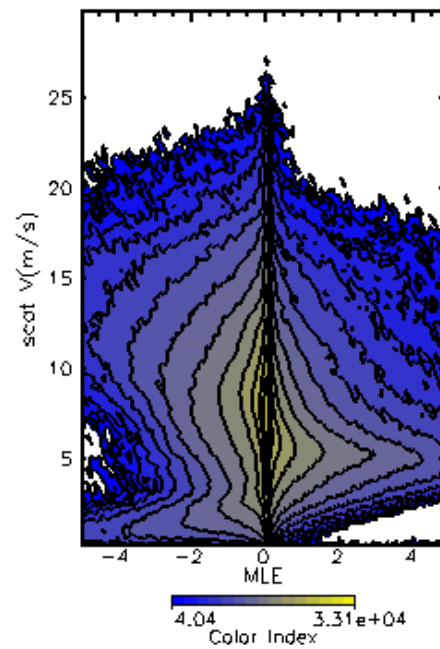
Figure 18 - MLE distribution per WVC shown. The data range is divided into 15 levels equally spaced on a log2 scale, each successive level is a factor of 2 higher than the previous level.
a) PPF550 corrected b) PPF550 uncorrected

Figure 19 shows the MLE as a function of the scatterometer wind speed for the PPF550 corrected and uncorrected cases. For high wind speed values the cone cross section is large compared to the spread of the triplets around the cone surface. A symmetrical pattern around the origin is expected here as an equal amount of triplets are on the inner and outer side of the cone surface (see Figure 10). For low wind speed values, i.e. smaller than ~ 4 m/s, the cone radius is small and the spread of triplets is relatively large. More triplets are expected to lie outside the cone and thus have a negative MLE. The visual correction moves the points on average towards more positive MLE values.

MLE vs V, PPF550 corr



MLE vs V, PPF550 uncorr



a)

b)

Figure 19 – Cone distance distribution versus measured wind speed
a) PPF550 corrected b) PPF550 uncorrected

Note that around 5 m/s most corrected triplets lie within the cone. This corresponds to earlier assessments that the CMOD5 cone is too wide for these winds [Portabella and Stoffelen, 2006]. After the ASCAT Cal/Val, we anticipate to use the MLE to correct CMOD5.n.

Routine monitoring statistics are accessible through the OSI SAF ASCAT product viewer web site:

http://www.knmi.nl/scatterometer/ascat_osi_25_prod/ascat_app.cgi

by selecting “Monitoring information”.

9 Conclusions

Based on the OSI SAF cone visualisation tools at KNMI and the CMOD5 wind sensitivity improved calibration of the ASCAT scatterometer is attempted. CMOD5 was carefully derived for the ERS scatterometer and thus our calibration should result in the compatibility of the ERS and ASCAT scatterometer products. Indeed, the scatterometer wind product of ASCAT is shown to have similar characteristics to the ERS scatterometer wind product and meets the wind product requirements.

ECMWF short range forecast winds are used here as reference. With the implementation of new ECMWF model cycles the ECMWF winds may become more or less biased. ECMWF verification statistics indicate that the low bias of ECMWF winds at the beginning of this century (e.g. [HERSBACH et al 2007]) have compensated by more recent ECMWF model cycles [HERSBACH, personal communication). Moreover, the random wind component errors in ECMWF and ERS scatterometer winds and their respective spatial representation are generally different. These differences may result in absolute overall biases of a few 10^{th} of a m/s; which results in a few 10^{th} of dB uncertainties in backscatter as well, however, rather uniformly spread over the WVCs [STOFFELEN 1999].

The ASCAT PPF550 three-transponder calibrated L1b backscatter data, is compared to the currently used PPF530 one-transponder calibrated L1b backscatter data. For the corrected case, consistency between the two sets is found, and the new "PPF550" set shows smaller interbeam differences suggesting improved L1b calibration. In the outer swath consistent large departures remain for the uncorrected case. The level 2 monitoring statistics, like average MLE, average wind speed bias with respect to the NWP wind speed, SD of the wind speed and wind direction show almost identical pictures for the PPF550 and PPF530 corrected data.

When using the correction table, the level 2 wind product is of high quality. The aim is to get also a high quality product without using a correction table. Of course, this could be easily achieved by incorporating the correction table in the CMOD fit-parameters. The current results from the ocean calibration for the uncorrected case are not acceptable for a level 2 wind product. This issue should be resolved by checking against other ancillary geophysical data like sea ice or rain forest. This will help in resolving any remaining errors in, and assessing the validity of the currently used CMOD version and L1b calibration, especially for the high incidence angles.

Appendix A1 – Visualisation correction factors

| # | WVC | visualisation correction in dB (fore, mid, aft) |
|----|---------------|---|
| 1 | -0.2836604714 | -1.5505601168 0.2836608589 |
| 2 | -0.2836604714 | -1.5505601168 0.2836608589 |
| 3 | -0.2836604714 | -1.5505601168 0.2836608589 |
| 4 | -0.2836604714 | -1.5505601168 0.2836608589 |
| 5 | -0.2836604714 | -1.5505601168 0.2836608589 |
| 6 | -0.2836604714 | -1.5505601168 0.2836608589 |
| 7 | -0.2836604714 | -1.5505601168 0.2836608589 |
| 8 | -0.2116521597 | -1.4642394781 0.2116516829 |
| 9 | -0.0698368698 | -1.3789786100 0.0698365122 |
| 10 | -0.0698368698 | -1.3789786100 0.0698365122 |
| 11 | 0.0691420585 | -1.3789786100 -0.0691419244 |
| 12 | 0.1715815663 | -1.0480247736 -0.1715817750 |
| 13 | 0.2725332081 | -0.8882772326 -0.2725330591 |
| 14 | 0.2053952366 | -0.4299544096 -0.2053952366 |
| 15 | 0.0691420585 | -0.4299544096 -0.0691419244 |
| 16 | -0.0698368698 | -0.5793946981 0.0698365122 |
| 17 | -0.1403827816 | -0.7321199775 0.1403826773 |
| 18 | -0.1403827816 | -0.8882772326 0.1403826773 |
| 19 | -0.2116521597 | -0.8882772326 0.2116516829 |
| 20 | -0.3564223349 | -1.0480247736 0.3564227819 |
| 21 | -0.3564223349 | -1.2115315199 0.3564227819 |
| 22 | 0.6622830629 | -1.0480247736 -0.6622830629 |
| 23 | 0.7874883413 | -1.1292968988 -0.7874885201 |
| 24 | 0.8492552042 | -0.8097600341 -0.8492550254 |
| 25 | 0.8492552042 | -0.3564223349 -0.8492550254 |
| 26 | 0.7251678705 | 0.0000000000 -0.7251676917 |
| 27 | 0.7874883413 | 0.3390282989 -0.7874885201 |
| 28 | 0.6622830629 | 0.4701407552 -0.6622830629 |
| 29 | 0.5347805023 | 0.3390282989 -0.5347801447 |
| 30 | 0.5347805023 | 0.1376028508 -0.5347801447 |
| 31 | 0.5025356412 | 0.0000000000 -0.5025355816 |
| 32 | 0.4701407552 | -0.1403827816 -0.4701409936 |
| 33 | 0.4048937261 | -0.3564223349 -0.4048934579 |
| 34 | 0.5347805023 | -0.5042726398 -0.5347801447 |
| 35 | 0.4701407552 | -0.5793946981 -0.4701409936 |
| 36 | 0.4701407552 | -0.6553375125 -0.4701409936 |
| 37 | 0.4701407552 | -0.6553375125 -0.4701409936 |
| 38 | 0.4701407552 | -0.6553375125 -0.4701409936 |
| 39 | 0.4701407552 | -0.7321199775 -0.4701409936 |
| 40 | 0.4701407552 | -0.9676917791 -0.4701409936 |
| 41 | 0.4701407552 | -1.1292968988 -0.4701409936 |
| 42 | 0.5025356412 | -1.2115315199 -0.5025355816 |

Appendix A2 – Wind speed bias correction tables - relative wind speed sensitivity

CMOD5 $(1/z) \cdot (dz/dV)$ at $V = 8$ m/s

| # one-sided WVC | fore | mid | aft |
|-----------------|----------|-----------|----------|
| 1 | 0.119159 | 0.0857779 | 0.119159 |
| 2 | 0.124659 | 0.0922501 | 0.124659 |
| 3 | 0.129497 | 0.0983018 | 0.129497 |
| 4 | 0.133716 | 0.103873 | 0.133716 |
| 5 | 0.137362 | 0.109056 | 0.137362 |
| 6 | 0.140481 | 0.113831 | 0.140481 |
| 7 | 0.143130 | 0.118247 | 0.143130 |
| 8 | 0.145348 | 0.122287 | 0.145348 |
| 9 | 0.147170 | 0.125973 | 0.147170 |
| 10 | 0.148632 | 0.129320 | 0.148632 |
| 11 | 0.149775 | 0.132372 | 0.149775 |
| 12 | 0.150622 | 0.135122 | 0.150622 |
| 13 | 0.151213 | 0.137606 | 0.151213 |
| 14 | 0.151568 | 0.139838 | 0.151568 |
| 15 | 0.151708 | 0.141815 | 0.151709 |
| 16 | 0.151658 | 0.143569 | 0.151658 |
| 17 | 0.151436 | 0.145113 | 0.151436 |
| 18 | 0.151060 | 0.146460 | 0.151060 |
| 19 | 0.150548 | 0.147634 | 0.150548 |
| 20 | 0.149904 | 0.148623 | 0.149904 |
| 21 | 0.149153 | 0.149459 | 0.149153 |

– wind speed bias for ss

WVC, scat Wind speed -NWP wind speed (m/s)

| | |
|----|-----------|
| 1 | -1.041865 |
| 2 | -0.850461 |
| 3 | -0.667734 |
| 4 | -0.493457 |
| 5 | -0.311385 |
| 6 | -0.175995 |
| 7 | -0.098697 |
| 8 | -0.011629 |
| 9 | 0.043326 |
| 10 | 0.128109 |
| 11 | 0.197760 |
| 12 | 0.262708 |
| 13 | 0.268704 |
| 14 | 0.187248 |
| 15 | 0.114800 |
| 16 | 0.109325 |
| 17 | 0.061379 |
| 18 | -0.151700 |
| 19 | -0.453545 |
| 20 | -0.646640 |
| 21 | -0.734591 |
| 22 | -1.029458 |
| 23 | -0.865391 |
| 24 | -0.659519 |
| 25 | -0.390793 |
| 26 | -0.100729 |
| 27 | 0.180286 |
| 28 | 0.391641 |
| 29 | 0.491469 |
| 30 | 0.519065 |
| 31 | 0.501218 |
| 32 | 0.413018 |
| 33 | 0.293345 |
| 34 | 0.150037 |
| 35 | 0.007671 |
| 36 | -0.154353 |
| 37 | -0.308192 |
| 38 | -0.463271 |
| 39 | -0.604827 |
| 40 | -0.725712 |
| 41 | -0.847465 |
| 42 | -0.982344 |

- wind speed bias correction factors for ss

| # Wind speed bias correction factors in dB | | | | |
|--|-----|-----------|-----------|-----------|
| # | WVC | fore | mid | aft |
| 1 | | 1.569614 | 1.573227 | 1.569614 |
| 2 | | 1.357468 | 1.344669 | 1.357468 |
| 3 | | 1.149168 | 1.125022 | 1.149168 |
| 4 | | 0.975064 | 0.943260 | 0.975064 |
| 5 | | 0.820573 | 0.784301 | 0.820573 |
| 6 | | 0.676105 | 0.638334 | 0.676105 |
| 7 | | 0.568740 | 0.530199 | 0.568744 |
| 8 | | 0.468421 | 0.431020 | 0.468421 |
| 9 | | 0.400052 | 0.363094 | 0.400052 |
| 10 | | 0.334474 | 0.299301 | 0.334474 |
| 11 | | 0.266030 | 0.234591 | 0.266030 |
| 12 | | 0.114930 | 0.099889 | 0.114931 |
| 13 | | 0.078903 | 0.067483 | 0.078903 |
| 14 | | 0.004670 | 0.003929 | 0.004670 |
| 15 | | 0.068210 | 0.056304 | 0.068210 |
| 16 | | 0.122410 | 0.099022 | 0.122410 |
| 17 | | 0.228750 | 0.180992 | 0.228750 |
| 18 | | 0.508881 | 0.392033 | 0.508881 |
| 19 | | 0.827278 | 0.618801 | 0.827278 |
| 20 | | 1.088548 | 0.788738 | 1.088548 |
| 21 | | 1.241614 | 0.870847 | 1.241614 |
| 22 | | 1.411981 | 0.986662 | 1.411981 |
| 23 | | 1.325342 | 0.955733 | 1.325342 |
| 24 | | 0.995430 | 0.742277 | 0.995430 |
| 25 | | 0.550349 | 0.423687 | 0.550349 |
| 26 | | 0.120715 | 0.095667 | 0.120715 |
| 27 | | -0.281540 | -0.229000 | -0.281540 |
| 28 | | -0.531137 | -0.441667 | -0.531137 |
| 29 | | -0.599706 | -0.507944 | -0.599706 |
| 30 | | -0.558416 | -0.480701 | -0.558416 |
| 31 | | -0.491500 | -0.429570 | -0.491503 |
| 32 | | -0.368874 | -0.327004 | -0.368874 |
| 33 | | -0.194323 | -0.174575 | -0.194323 |
| 34 | | -0.017210 | -0.015663 | -0.017210 |
| 35 | | 0.161933 | 0.149265 | 0.161933 |
| 36 | | 0.350777 | 0.327355 | 0.350779 |
| 37 | | 0.516439 | 0.487903 | 0.516439 |
| 38 | | 0.685344 | 0.655335 | 0.685344 |
| 39 | | 0.874740 | 0.846411 | 0.874740 |
| 40 | | 1.093792 | 1.070901 | 1.093792 |
| 41 | | 1.284003 | 1.271961 | 1.284003 |
| 42 | | 1.465337 | 1.468684 | 1.465337 |

Appendix A3 – Normalisation correction tables

- PPF550 to PPF530

The PF550 to PPF530 calibration correction factors (dB) as a function of WVC and beam:

| # | WVC | diff_sigma0 (dB) fore | mid | aft |
|-----|-----|-----------------------|--------------|--------------|
| 1. | | 0.2714430690 | 0.5549128056 | 0.2714430690 |
| 2. | | 0.3093338907 | 0.5461968184 | 0.3093338907 |
| 3. | | 0.3445208073 | 0.5134129524 | 0.3445208073 |
| 4. | | 0.3691216409 | 0.4556634724 | 0.3691216409 |
| 5. | | 0.3819622099 | 0.4036121964 | 0.3819622099 |
| 6. | | 0.3787407577 | 0.3800781667 | 0.3787407577 |
| 7. | | 0.3620991707 | 0.3881050348 | 0.3620991707 |
| 8. | | 0.3396820426 | 0.4153954387 | 0.3396820426 |
| 9. | | 0.3242164254 | 0.4416214228 | 0.3242164254 |
| 10. | | 0.3261019289 | 0.4486402273 | 0.3261019289 |
| 11. | | 0.3496892750 | 0.4321569502 | 0.3496892750 |
| 12. | | 0.3884899020 | 0.4065565467 | 0.3884899020 |
| 13. | | 0.4311251342 | 0.3950270712 | 0.4311251342 |
| 14. | | 0.4581308663 | 0.4124276638 | 0.4581308663 |
| 15. | | 0.4428449571 | 0.4546571970 | 0.4428449571 |
| 16. | | 0.3773616552 | 0.4958844781 | 0.3773616552 |
| 17. | | 0.2870293558 | 0.5099437237 | 0.2870293558 |
| 18. | | 0.2124268860 | 0.5012078285 | 0.2124268860 |
| 19. | | 0.1982158720 | 0.5148668289 | 0.1982158720 |
| 20. | | 0.2375109345 | 0.6077215075 | 0.2375109345 |
| 21. | | 0.2667729259 | 0.7645369172 | 0.2667729259 |
| 22. | | 0.3348593116 | 0.6600804925 | 0.3348593116 |
| 23. | | 0.2790255845 | 0.4048612416 | 0.2790255845 |
| 24. | | 0.2388466001 | 0.2680703402 | 0.2388466001 |
| 25. | | 0.2378155887 | 0.2691104412 | 0.2378155887 |
| 26. | | 0.2652266324 | 0.3318253160 | 0.2652266324 |
| 27. | | 0.3008913100 | 0.3808834255 | 0.3008913100 |
| 28. | | 0.3326663673 | 0.3937389851 | 0.3326663673 |
| 29. | | 0.3553055823 | 0.3885897696 | 0.3553055823 |
| 30. | | 0.3696043491 | 0.3926064372 | 0.3696043491 |
| 31. | | 0.3788559139 | 0.4165528417 | 0.3788559139 |
| 32. | | 0.3822078705 | 0.4463786185 | 0.3822078705 |
| 33. | | 0.3832875490 | 0.4532978833 | 0.3832875490 |
| 34. | | 0.3839687109 | 0.4189292192 | 0.3839687109 |
| 35. | | 0.3839487135 | 0.3507410884 | 0.3839487135 |
| 36. | | 0.3795850277 | 0.2784701884 | 0.3795850277 |
| 37. | | 0.3683530390 | 0.2382061779 | 0.3683530390 |
| 38. | | 0.3493097723 | 0.2571823299 | 0.3493097723 |
| 39. | | 0.3266015351 | 0.3354217410 | 0.3266015351 |
| 40. | | 0.3033074439 | 0.4379919767 | 0.3033074439 |
| 41. | | 0.2858630717 | 0.4990984797 | 0.2858630717 |
| 42. | | 0.2719370723 | 0.4743648767 | 0.2719370723 |

- PPF530 to zzz

The PPF530 to zzz calibration correction factors (dB) as a function of WVC and beam:

| # wvc | diff_sigma0(dB) fore | mid | aft |
|-------|----------------------|---------------|---------------|
| 1. | -0.0370333903 | -0.3018574119 | -0.0372132584 |
| 2. | -0.0867435783 | -0.1729753613 | -0.1677785069 |
| 3. | -0.1342121810 | -0.1076786891 | -0.2142298371 |
| 4. | -0.1691072881 | -0.0690770745 | -0.1988888681 |
| 5. | -0.1898018420 | -0.0630657524 | -0.1567329168 |
| 6. | -0.1912569404 | -0.0945294574 | -0.1124063209 |
| 7. | -0.1736918539 | -0.1553879231 | -0.0836619660 |
| 8. | -0.1454696804 | -0.2254291773 | -0.0820216015 |
| 9. | -0.1190418303 | -0.2790581286 | -0.1102506518 |
| 10. | -0.1086801440 | -0.2909408510 | -0.1660518944 |
| 11. | -0.1206367612 | -0.2525698245 | -0.2392058820 |
| 12. | -0.1530949324 | -0.1781437248 | -0.3116568923 |
| 13. | -0.2002111375 | -0.0964003950 | -0.3622547388 |
| 14. | -0.2460798621 | -0.0334451608 | -0.3746898174 |
| 15. | -0.2614217997 | -0.0057791495 | -0.3328388631 |
| 16. | -0.2275087386 | -0.0205562748 | -0.2252153009 |
| 17. | -0.1407288760 | -0.0658641607 | -0.0625925735 |
| 18. | -0.0202942006 | -0.1198330373 | 0.1103230864 |
| 19. | 0.0854148120 | -0.1659138501 | 0.2220056653 |
| 20. | 0.1338241398 | -0.1978767663 | 0.1964467764 |
| 21. | 0.0835229233 | -0.1959892809 | -0.0231189765 |
| 22. | -0.3135213554 | -0.3128969967 | -0.2646456063 |
| 23. | 0.2065495700 | -0.3155142665 | 0.3543663025 |
| 24. | 0.1713631749 | -0.1163798422 | 0.4794062078 |
| 25. | -0.0218976960 | 0.0815279260 | 0.3568073809 |
| 26. | -0.2170903534 | 0.2072746009 | 0.1454687417 |
| 27. | -0.3365450203 | 0.2527061999 | -0.0458683409 |
| 28. | -0.3659032583 | 0.2346272320 | -0.1675790399 |
| 29. | -0.3257602751 | 0.1640122384 | -0.2125920802 |
| 30. | -0.2513826191 | 0.0572210178 | -0.2063862085 |
| 31. | -0.1767978370 | -0.0498710796 | -0.1741460264 |
| 32. | -0.1186584085 | -0.1249945834 | -0.1336213797 |
| 33. | -0.0867970437 | -0.1425857395 | -0.0997030586 |
| 34. | -0.0815665275 | -0.1009307429 | -0.0823161006 |
| 35. | -0.0961823165 | -0.0251438916 | -0.0811731592 |
| 36. | -0.1188202873 | 0.0448322110 | -0.0902518630 |
| 37. | -0.1386291981 | 0.0712327287 | -0.1033248827 |
| 38. | -0.1469563544 | 0.0320821814 | -0.1164994761 |
| 39. | -0.1426671296 | -0.0670931265 | -0.1258317828 |
| 40. | -0.1259345114 | -0.1822225451 | -0.1312264353 |
| 41. | -0.1009131819 | -0.2413870096 | -0.1304559410 |
| 42. | -0.0660245270 | -0.1951905638 | -0.1168597117 |

- zzz to zz

```

# zzz-zz per WVC, sigfore, sigmid, sigaft
 1  0.0243748464 -0.0033332903 0.1477082968
 2 -0.0402082391 -0.1643749028 0.1902081817
 3 -0.0887499526 -0.2291665971 0.2172916830
 4 -0.1185418442 -0.2352083474 0.2310415506
 5 -0.1374998987 -0.2135416120 0.2337499112
 6 -0.1433332115 -0.1804165393 0.2235416323
 7 -0.1402084529 -0.1508332789 0.2016668022
 8 -0.1289583147 -0.1270834804 0.1724999845
 9 -0.1079166755 -0.1127082855 0.1356248707
10 -0.0822916552 -0.1024999693 0.0949999616
11 -0.0535415784 -0.0891666934 0.0564582758
12 -0.0189582910 -0.0683333278 0.0239582863
13  0.0154165421 -0.0320832506 0.0039584036
14  0.0522916876  0.0279165544 0.0006249944
15  0.0902083889  0.1087499857 0.0222915802
16  0.1289582253  0.2054166347 0.0749999955
17  0.1752082556  0.2979166508 0.1656250060
18  0.2312500030  0.3718750477 0.3072914481
19  0.3133332431  0.4056249559 0.5120832920
20  0.4452083111  0.3706250489 0.8112499714
21  0.6649999619  0.2675000727 1.2452085018
22  1.9952083826  0.7999998927 1.7406249046
23  1.4435416460  0.8027083278 0.9791665673
24  1.2383333445  0.7074999213 0.5647916198
25  1.0525003672  0.5577083230 0.3314582705
26  0.8247916102  0.3952084482 0.1895833313
27  0.5785415769  0.2458332926 0.1010416746
28  0.3364583254  0.1218750477 0.0462499894
29  0.1310416609  0.0327083319 0.0139582967
30 -0.0177082997 -0.0147917457 -0.0004166563
31 -0.1143750101 -0.0245835353 -0.0047916374
32 -0.1595833451 -0.0035416684 -0.0018750230
33 -0.1652082950  0.0420833454 0.0054166522
34 -0.1429166645  0.1033333763 0.0156249395
35 -0.1049999371  0.1729166806 0.0239583664
36 -0.0591667369  0.2424999774 0.0322916731
37 -0.0183332767  0.3016666174 0.0385416821
38  0.0139582744  0.3406250477 0.0429167263
39  0.0252083912  0.3531248868 0.0468750447
40  0.0191666521  0.3289583325 0.0481250547
41 -0.0077083716  0.2599999309 0.0497915782
42 -0.0564584509  0.1420833021 0.0500000231

```

- ZZ to SS

```

# zz-ss per WVC, sigfore, sigmid, sigaft
 1  0.0482655130 -0.2895376086  0.6462509036
 2  0.0593577623 -0.3686678112  0.6049097776
 3  0.0677057356 -0.4443484843  0.5659368038
 4  0.0773898736 -0.5172165036  0.5282182693
 5  0.0914745107 -0.5858699083  0.4860347509
 6  0.1076411679 -0.6473990083  0.4468710423
 7  0.1287017763 -0.6976425648  0.4115951359
 8  0.1487030834 -0.7344702482  0.3729788661
 9  0.1571636498 -0.7553432584  0.3270730674
10  0.1674532294 -0.7559102774  0.2782683074
11  0.1804929376 -0.7317994237  0.2388679087
12  0.1986887008 -0.6877077818  0.2135602683
13  0.2060010880 -0.6416571140  0.2025974393
14  0.2004764080 -0.6149933934  0.2099165469
15  0.1861767918 -0.6240960360  0.2348827422
16  0.1660306156 -0.6510289311  0.2781338990
17  0.1424836814 -0.6563382745  0.3322808146
18  0.1220258325 -0.6377570033  0.3863241076
19  0.1111740917 -0.6209232211  0.4184640646
20  0.1136913672 -0.6130168438  0.4009121656
21  0.1348361969 -0.5943609476  0.3381395638
22  0.3508432508 -0.5647418499 -0.7795034647
23  0.4270028770 -0.5816165209 -0.6958812475
24  0.4274401963 -0.6120569110 -0.7022020221
25  0.3565745652 -0.6305339932 -0.7866245508
26  0.2482697964 -0.6284136176 -0.9179996252
27  0.1452310830 -0.6099900007 -1.0538300276
28  0.0669959411 -0.5963429213 -1.1511170864
29  0.0313193686 -0.6015726924 -1.1864163876
30  0.0382982418 -0.6231390834 -1.1651347876
31  0.0803977028 -0.6583665013 -1.1091285944
32  0.1479337364 -0.6935549974 -1.0325934887
33  0.2239565998 -0.7170857191 -0.9415782094
34  0.3068754971 -0.7211312652 -0.8362450004
35  0.3941792548 -0.7053554058 -0.7209556699
36  0.4790285528 -0.6716300845 -0.6141123176
37  0.5615235567 -0.6244813204 -0.5137995481
38  0.6431853771 -0.5696477294 -0.4197139740
39  0.7232847810 -0.5091590285 -0.3285492957
40  0.7982527614 -0.4447305799 -0.2317700535
41  0.8733042479 -0.3786087334 -0.1357937753
42  0.9467259049 -0.3112885952 -0.0479744412

```


Appendix A4 – Total correction tables – total for PPF550

The total calibration correction factors (dB) as a function of WVC and beam:

total correction factors in dB for PPF550

| # WVC | fore | mid | aft |
|-------|--------------|--------------|--------------|
| 1 | 0.978903592 | 0.062482476 | 0.723580241 |
| 2 | 0.832067609 | -0.046069860 | 0.550660729 |
| 3 | 0.676243067 | -0.157757252 | 0.384414822 |
| 4 | 0.532541037 | -0.241461664 | 0.255324483 |
| 5 | 0.390777439 | -0.307394028 | 0.154008567 |
| 6 | 0.240652770 | -0.369959325 | 0.066826910 |
| 7 | 0.108178914 | -0.404602468 | 0.019773394 |
| 8 | 0.042811722 | -0.361631989 | -0.082582295 |
| 9 | 0.075793594 | -0.310396403 | -0.206639975 |
| 10 | -0.037946254 | -0.378966719 | -0.173441172 |
| 11 | -0.020831823 | -0.503008664 | -0.284991354 |
| 12 | -0.128613800 | -0.420507491 | -0.453169137 |
| 13 | -0.100895435 | -0.445680499 | -0.527272999 |
| 14 | -0.254753888 | -0.217931077 | -0.513653159 |
| 15 | -0.320456296 | -0.307182401 | -0.359835774 |
| 16 | -0.392268628 | -0.510088623 | -0.309107244 |
| 17 | -0.375625193 | -0.636785924 | -0.387221724 |
| 18 | -0.176910311 | -0.611737013 | -0.456692874 |
| 19 | -0.092512161 | -0.403130919 | -0.443357795 |
| 20 | -0.198109105 | -0.426739693 | -0.356662869 |
| 21 | -0.264940321 | -0.582371235 | -0.410173267 |
| 22 | -0.293125540 | -0.643804312 | -0.187478855 |
| 23 | -0.243289277 | -0.484002680 | -0.256246656 |
| 24 | -0.231298119 | -0.314616501 | -0.309868336 |
| 25 | -0.225388616 | -0.210548013 | -0.334783971 |
| 26 | -0.275314808 | -0.210227743 | -0.226409718 |
| 27 | -0.182170644 | -0.159404635 | -0.363593042 |
| 28 | -0.239071310 | -0.125424623 | -0.291819096 |
| 29 | -0.256831825 | -0.152653351 | -0.169162601 |
| 30 | -0.162447184 | -0.154994786 | -0.162806541 |
| 31 | -0.157045126 | -0.113301694 | -0.149751484 |
| 32 | -0.150633126 | -0.091674149 | -0.103538990 |
| 33 | -0.144668072 | -0.166707069 | 0.018360287 |
| 34 | 0.051209509 | -0.220136225 | -0.060597301 |
| 35 | 0.055128068 | -0.223288208 | 0.058017343 |
| 36 | 0.140291154 | -0.222154811 | 0.136535943 |
| 37 | 0.213665694 | -0.154058725 | 0.206970245 |
| 38 | 0.295987636 | -0.060244337 | 0.292931557 |
| 39 | 0.412453264 | 0.001996547 | 0.405505508 |
| 40 | 0.569140315 | -0.036787927 | 0.546004891 |
| 41 | 0.703598022 | 0.003561437 | 0.659630060 |
| 42 | 0.871692717 | 0.147183418 | 0.744379520 |

– total for PPF530

The total calibration correction factors (dB) as a function of WVC and beam:

total correction factors in dB for PPF530

| # WVC | fore | mid | aft |
|-------|--------------|--------------|--------------|
| 1 | 1.2503467 | 0.6173953 | 1.0965289 |
| 2 | 1.1414015 | 0.50012696 | 1.0137894 |
| 3 | 1.0207639 | 0.3556557 | 0.8638302 |
| 4 | 0.9016627 | 0.21420181 | 0.6983539 |
| 5 | 0.77273965 | 0.096218154 | 0.5411821 |
| 6 | 0.6193935 | 0.01011885 | 0.40175956 |
| 7 | 0.47027808 | -0.016497448 | 0.32280484 |
| 8 | 0.38249376 | 0.05376345 | 0.21661538 |
| 9 | 0.40001002 | 0.13122502 | 0.11744121 |
| 10 | 0.28815567 | 0.06967351 | 0.19709414 |
| 11 | 0.32885745 | -0.07085171 | 0.14076778 |
| 12 | 0.2598761 | -0.013950959 | 0.017487556 |
| 13 | 0.3302297 | -0.050653443 | -0.037931174 |
| 14 | 0.203377 | 0.19449659 | -0.036576986 |
| 15 | 0.12238866 | 0.1474748 | 0.0747326 |
| 16 | -0.014906973 | -0.014204141 | 0.06432791 |
| 17 | -0.08859584 | -0.12684219 | -0.06618055 |
| 18 | 0.03551657 | -0.1105292 | -0.15467502 |
| 19 | 0.10570371 | 0.11173591 | -0.11362332 |
| 20 | 0.03940183 | 0.18098183 | 0.036361814 |
| 21 | 0.001832597 | 0.18216565 | 0.037807677 |
| 22 | 0.04173377 | 0.016276151 | 0.05322209 |
| 23 | 0.035736308 | -0.07914144 | -0.09979808 |
| 24 | 0.007548481 | -0.046546176 | -0.19582084 |
| 25 | 0.012426965 | 0.05856242 | -0.20054713 |
| 26 | -0.010088161 | 0.12159757 | -0.021505147 |
| 27 | 0.118720666 | 0.22147879 | -0.07037181 |
| 28 | 0.09359506 | 0.26831436 | 0.07902609 |
| 29 | 0.09847376 | 0.23593642 | 0.25056392 |
| 30 | 0.20715716 | 0.23761165 | 0.27874148 |
| 31 | 0.22181079 | 0.30325115 | 0.29402766 |
| 32 | 0.23157474 | 0.35470447 | 0.32907492 |
| 33 | 0.23861948 | 0.2865908 | 0.4366482 |
| 34 | 0.43517822 | 0.198793 | 0.350946 |
| 35 | 0.43907678 | 0.12745288 | 0.46996248 |
| 36 | 0.5198762 | 0.05631538 | 0.55271053 |
| 37 | 0.58201873 | 0.08414746 | 0.6248808 |
| 38 | 0.6452974 | 0.196938 | 0.7084997 |
| 39 | 0.7390548 | 0.3374183 | 0.812105 |
| 40 | 0.8724477 | 0.40120405 | 0.9385224 |
| 41 | 0.98946106 | 0.5026599 | 1.0303202 |
| 42 | 1.1436298 | 0.6215483 | 1.0776356 |

– total for zzz

The total calibration correction factors as a function of WVC and beam:

total correction factors in dB for zzz:

| # WVC | fore | mid | aft |
|-------|---------------|---------------|---------------|
| 1 | 1.2133132219 | 0.3155378401 | 1.0593156815 |
| 2 | 1.0546579361 | 0.3271515965 | 0.8460109234 |
| 3 | 0.8865517378 | 0.2479770184 | 0.6496003866 |
| 4 | 0.7325554490 | 0.1451247334 | 0.4994649887 |
| 5 | 0.5829378366 | 0.0331524014 | 0.3844491839 |
| 6 | 0.4281365871 | -0.0844106078 | 0.2893532515 |
| 7 | 0.2965862155 | -0.1718853712 | 0.2391428649 |
| 8 | 0.2370240837 | -0.1716657281 | 0.1345937848 |
| 9 | 0.2809681892 | -0.1478331089 | 0.0071905553 |
| 10 | 0.1794755459 | -0.2212673426 | 0.0310422480 |
| 11 | 0.2082206905 | -0.3234215379 | -0.0984380990 |
| 12 | 0.1067811698 | -0.1920946836 | -0.2941693366 |
| 13 | 0.1300185770 | -0.1470538378 | -0.4001859128 |
| 14 | -0.0427028686 | 0.1610514224 | -0.4112668037 |
| 15 | -0.1390331388 | 0.1416956484 | -0.2581062615 |
| 16 | -0.2424157113 | -0.0347604156 | -0.1608873904 |
| 17 | -0.2293247133 | -0.1927063465 | -0.1287731230 |
| 18 | 0.0152223706 | -0.2303622365 | -0.0443519354 |
| 19 | 0.1911185235 | -0.0541779399 | 0.1083823442 |
| 20 | 0.1732259691 | -0.0168949366 | 0.2328085899 |
| 21 | 0.0853555202 | -0.0138236284 | 0.0146887004 |
| 22 | -0.2717875838 | -0.2966208458 | -0.2114235163 |
| 23 | 0.2422858775 | -0.3946557045 | 0.2545682192 |
| 24 | 0.1789116561 | -0.1629260182 | 0.2835853696 |
| 25 | -0.0094707310 | 0.1400903463 | 0.1562602520 |
| 26 | -0.2271785140 | 0.3288721740 | 0.1239635944 |
| 27 | -0.2178243548 | 0.4741849899 | -0.1162401438 |
| 28 | -0.2723082006 | 0.5029416084 | -0.0885529518 |
| 29 | -0.2272865176 | 0.3999486566 | 0.0379718542 |
| 30 | -0.0442254469 | 0.2948326766 | 0.0723552704 |
| 31 | 0.0450129583 | 0.2533800602 | 0.1198816299 |
| 32 | 0.1129163355 | 0.2297098935 | 0.1954535246 |
| 33 | 0.1518224329 | 0.1440050602 | 0.3369451165 |
| 34 | 0.3536116779 | 0.0978622437 | 0.2686299086 |
| 35 | 0.3428944647 | 0.1023089886 | 0.3887893260 |
| 36 | 0.4010559022 | 0.1011475921 | 0.4624586403 |
| 37 | 0.4433895350 | 0.1553801894 | 0.5215559006 |
| 38 | 0.4983410835 | 0.2290201783 | 0.5920002460 |
| 39 | 0.5963876843 | 0.2703251541 | 0.6862732172 |
| 40 | 0.7465131879 | 0.2189815044 | 0.8072959781 |
| 41 | 0.8885478973 | 0.2612728775 | 0.8998641968 |
| 42 | 1.0776052475 | 0.4263577461 | 0.9607759118 |

Acronyms and abbreviations

| Name | Description |
|-------------|--|
| AMI | Active Microwave Instrument |
| ASCAT | Advanced scatterometer |
| AWDP | Ascat Wind Data Processor |
| BUFR | Binary Universal Form for Representation (of meteorological data) |
| CMOD | C-band geophysical model function used for ERS and ASCAT |
| ECMWF | European Centre for Medium-Range Weather Forecasts |
| ERA40 | ECMWF 40 year reanalysis |
| ERS | European Remote sensing Satellite |
| ESA | European Space Agency |
| ESDP | ERS Scatterometer Data Processor |
| EUMETSAT | European Organization for the Exploitation of Meteorological Satellites |
| GMF | geophysical model function |
| KNMI | Koninklijk Nederlands Meteorologisch Instituut (Royal Netherlands Meteorological Institute) |
| METOP | Meteorological Operational satellite |
| MLE | maximum likelihood estimator (used for distance to cone) |
| NWP | numerical weather prediction |
| OSI | Ocean and Sea Ice |
| QC | Quality Control (inversion and ambiguity removal) |
| SAF | Satellite Application Facility |
| SD | standard deviation |
| WVC | wind vector cell, also known as node or cell |

Table 1 - List of acronyms and abbreviations

References

[FIGA 2004] Figa-Saldaña, Julia, "ASCAT calibration and validation plan", *EUMETSAT*, EPS programme, Darmstadt Germany, 2004

[FIGA et al 2002] Figa-Saldaña, J., J.J.W. Wilson, E. Attema, R. Gelsthorpe, M.R. Drinkwater, and A. Stoffelen, The Advanced scatterometer (ASCAT) on the meteorological operational (MetOp) platform: A follow on for the European wind scatterometers, *Can. J. Remote Sensing* **28** (3), pp. 404-412, 2002.

[HERSBACH 2003] Hersbach, Hans, "CMOD5 An improved geophysical model function for ERS C-band scatterometry, *Technical Memorandum 395*, *ECMWF*, Reading GB, 2003

[HERSBACH et al 2007] Hans Hersbach, Ad Stoffelen, Siebren de Haan, CMOD5, *J. Geophys. Res.*, accepted.

[PORTABELLA and STOFFELEN 2006] Marcos Portabella, Ad Stoffelen, Scatterometer backscatter uncertainty due to wind variability, *IEEE Trans. Geosci. Rem. Sens.* **44** (11), 3356-3362, 2006.

[PORTABELLA and STOFFELEN 2007] Portabella, M., and Stoffelen, A., "On scatterometer ocean stress," submitted to *J. Atm. and Ocean Techn.* in June 2007, © American Meteorological Society

[STOFFELEN 1999] Stoffelen, Ad, "A Simple Method for Calibration of a Scatterometer over the Ocean", *J. Atm. and Ocean Techn.* **16**(2), 275-282, 1999.

[STOFFELEN 1998] Stoffelen, Ad, "Scatterometry", KNMI, *PhD thesis at the University of Utrecht*, ISBN 90-39301708-9, October 1998

[STOFFELEN and ANDERSON 1997] Stoffelen, Ad, and David Anderson, "Scatterometer Data Interpretation: Measurement Space and inversion", *J. Atm. and Ocean Techn.*, **14**(6), 1298-1313, 1997.

[VERSPEEK 2006] Verspeek, Jeroen, "Scatterometer calibration tool development", *EUMETSAT Technical Report SAF/OSI/KNMI/TEC/RP/092*, *KNMI*, de Bilt, 2006,

[VERSPEEK 2006-2] Verspeek, Jeroen, "User manual Measurement space visualisation package", *KNMI*, de Bilt, 2006